An overview of Alpine and Mediterranean palaeogeography, terrestrial ecosystems and climate history during MIS 3 with focus on the Middle to Upper Palaeolithic transition

(Article begins on next page)

23 June 2024

Journal Pre-proof

An overview of Alpine and Mediterranean palaeogeography, terrestrial ecosystems and climate history during MIS 3 with focus on the Middle to Upper Palaeolithic transition

Federica Badino, Roberta Pini, Cesare Ravazzi, Davide Margaritora, Simona Arrighi, Eugenio Bortolini, Carla Figus, Biagio Giaccio, Federico Lugli, Giulia Marciani, Giovanni Monegato, Adriana Moroni, Fabio Negrino, Gregorio Oxilia, Marco Peresani, Matteo Romandini, Annamaria Ronchitelli, Enza E. Spinapolice, Andrea Zerboni, Stefano Benazzi

1

An overview of Alpine and Mediterranean palaeogeography,

terrestrial ecosystems and climate history during MIS 3

with focus on the Middle to Upper Palaeolithic transition

5

Federica Badino[a,b,*], Roberta Pini[b], Cesare Ravazzi[b], Davide Margaritora[b], Simona Arrighi[a,c,d],

Eugenio Bortolini[a], Carla Figus[a], Biagio Giaccio[b], Federico Lugli[a,e], Giulia Marciani[a,d], Giovanni

Monegato[f], Adriana Moroni[c], Fabio Negrino[g], Gregorio Oxilia[a], Marco Peresani[h], Matteo

Romandini[a,h], Annamaria Ronchitelli[c], Enza E. Spinapolice[i], Andrea Zerboni[j], Stefano Benazzi[a,k]

[a] Dipartimento di Beni Culturali, Università di Bologna, 48121 Ravenna, Italy

[b] C.N.R. - Istituto di Geologia Ambientale e Geoingegneria, 20126 Milano, Italy

[c] Dipartimento di Scienze Fisiche della Terra e dell'Ambiente, Università di Siena, 53100 Siena, Italy

[d] Centro Studi sul Quaternario, 52037 Sansepolcro, Italy

[e] Dipartimento di Scienze Chimiche e Geologiche, Università di Modena e Reggio Emilia, 41125 Modena,
Italy

[f] C.N.R. - Istituto di Geoscienze e Georisorse, 35131 Padova, Italy

[g] Dipartimento Antichità, Filosofia e Storia, Università di Genova, 16126 Genova, Italy

[h] Dipartimento di Studi Umanistici, Sezione di Scienze Preistoriche e Antropologiche, Università di Ferrara,
44100 Ferrara, Italy

[i] Dipartimento di Scienze dell'Antichità, Università Sapienza, 00185 Roma, Italy

[j] Dipartimento di Scienze della Terra "A. Desio", Università degli Studi di Milano, 20133 Milano, Italy

[k] Department of Human Evolution Max Planck Institute for Evolutionary Anthropology, 04103 Leipzig,
Germany

24

* Corresponding author: Federica Badino federica.badino@unibo.it

26 Università di Bologna

27 Dipartimento di Beni Culturali

28 Via degli Ariani 1

29 48121 Ravenna (Italy)

30 http://www.erc-success.eu/

31

Abstract

33 This paper summarizes the current state of knowledge about the millennial scale climate

34 variability characterizing Marine Isotope Stage 3 (MIS 3) in S-Europe and the

35 Mediterranean area and its effects on terrestrial ecosystems. The sequence of Dansgaard-

36 Oeschger events, as recorded by Greenland ice cores and recognizable in isotope profiles

37 from speleothems and high-resolution palaeoecological records, led to dramatic variations

38 in glacier extent and sea level configuration with major impacts on the physiography and

39 vegetation patterns, both latitudinally and altitudinally. The recurrent succession of (open)

40 woodlands, including temperate taxa, and grasslands with xerophytic elements, have been

41 tentatively correlated to GIs in Greenland ice cores. Concerning colder phases, the

42 Greenland Stadials (GSs) related to Heinrich events (HEs) appear to have a more

43 pronounced effect than other GSs on woodland withdrawal and xerophytes expansion.

44 Notably, GS 9-HE4 phase corresponds to the most severe reduction of tree cover in a

45 number of Mediterranean records. On a long-term scale, a reduction/opening of forests

46 throughout MIS 3 started from Greenland Interstadials (GIs) 14/ 13 (ca. 55-48 ka), showing

47 a maximum in woodland density. At that time, natural environments were favourable for

48 Anatomically Modern Humans (AMHs) to migrate from Africa into Europe as documented

49 by industries associated with modern hominin remains in the Levant. Afterwards, a variety

50 of early Upper Palaeolithic cultures emerged (e.g., Uluzzian and Proto-Aurignacian). In this

51 chronostratigraphic framework, attention is paid to the Campanian Ignimbrite tephra

52 marker, as a pivotal tool for deciphering and correlating several temporal-spatial issues

53 crucial for understanding the interaction between AMHs and Neandertals at the time of the

54 Middle to Upper Palaeolithic transition.

55 **Keywords**: Middle Upper Palaeolithic, Palaeoecology, Palaeoclimate, Marine Isotope

56 Stage 3, Terrestrial records

57

58 1 Introduction

59 Climate variability and landscape transformations underlie the complex interaction

60 between natural resources and human dynamics. The understanding of these changes

61 over time relies on palaeoclimate and palaeoecological information obtained from different

62 natural archives (e.g. terrestrial and marine sediments, speleothems, ice cores, etc.),

63 which are well known for their potential to record even abrupt and high frequencies events.

64 The Marine Isotope Stage 3 (MIS 3) in the Last Glacial Period (Lisiecki and Raymo, 2005)

65 is one of the most highly unstable phases, as far as climate is concerned, closely

66 interwoven with the recent human evolution history. MIS 3 (ca. 60-30 ka) was

67 characterized by major rapid climatic changes showing high variability, associated with

68 abrupt atmospheric shifts over Greenland (Dansgaard-Oeschger [D-O] events) and

69 episodes of massive iceberg discharge into the North Atlantic (Heinrich events [HEs]),

3

70 enhancing cold and dry conditions at mid-to-low latitudes (Fletcher and Sánchez Goñi,

71 2008; Fleitmann et al., 2009; Naughton et al., 2009; Fletcher et al., 2010a).

72 Within this context, the Middle to Upper Palaeolithic transition (ca. 50-30 ka in Europe and

73 western Asia, Higham et al. 2014; Benazzi et al., 2015; Hublin 2015; Douka and Higham,

74 2017; Been et al., 2017; Margherita et al., 2017) represents one of the pivotal phases in

75 human evolution documenting the demise of the autochthonous Neandertals and their

76 replacement by Anatomically Modern Humans (AMHs). Many authors suggest that the

77 eastern Mediterranean region and, in turn, the Italian Peninsula, served as gateways for

78 the immigration and spread of AMHs from Africa to western Eurasia (van Andel et al.,

79 2003; Müller et al., 2011; Moroni et al., 2013; 2018), where various transitional

80 technocomplexes (eg., the Uluzzian in Italy and Greece, the Châtelperronian in central and

81 south western France and northern Spain, the Neronian in south eastern France) replaced

82 pre-existing Mousterian cultures (Mellars, 2006). Neandertals and AMHs societies

83 developed in a context of continuous climatic fluctuations between cold-arid (Greenland

84 Stadial, GS) and mild-humid (Greenland Interstadial, GI) conditions (Staubwasser et al.,

85 2018). Surprisingly, despite the apparent body adaptations to live under rigid climates

86 conditions (Steegmann et al., 2002), e.g., a wide and tall nasal aperture useful in

87 humidifying and warming cold and dry air (Franciscus, 1999; Wroe et al., 2018),

88 Neandertals did not survive into the coldest phases of MIS 3. Their extinction is statistically

89 placed around 40 ka cal BP (Higham et al., 2014) and almost in coincidence with

90 Greenland Stadial 9/HE 4, which is a noticeable cold phase recorded in both marine and

91 terrestrial records (e.g. Fedele et al, 2003; Guellevic et al., 2014 and references therein).

92 Several hypotheses have been proposed about Neandertal extinction and AMHs

93 replacement, and the debate is still unresolved (e.g., Mellars 2006; Hoffecker 2009;

94 Benazzi et al., 2011; 2015; Villa and Roebroeks, 2014; Higham et al., 2014; Hublin, 2015;

95 Rey-Rodríguez et al., 2016; Greenbaum et al., 2018).

96 To disentangle the role played by climate, ecosystem changes and physiography in such

97 human processes, a palaeoclimate and palaeoecological perspective focusing on Europe

98 and the Mediterranean area is essential. These efforts represent part of a wider interest in

99 determining how abrupt climate changes modified past environments.

100 The aim of this paper is to present the state-of-the-art of palaeoclimate and

101 palaeoecological researches relevant to the ERC Consolidator Grant 2016 "SUCCESS -

102 *The earliest migration of Homo sapiens in southern Europe: understanding the biocultural*

103 *processes that define our uniqueness*". To contribute to the discussion about the arrival of

104 AMHs in Southern Europe, the pattern of their diffusion and their interactions with

105 Neandertals, a review of the current knowledge about the climate context and the

106 landscape structure is presented. A selection of high-resolution palaeoecological records

107 covering the time span between HE 5 to 3, known for their strong impact in western

108 Eurasia, are discussed to explore the effects of short-term climate variability on

109 ecosystems and human interactions.

110

2 Reference climate records for the Last Glacial period and signal synchronicity between different realms

2.1 MIS 3 as recorded in Greenland ice cores

MIS 3, which lasted from 60 ka to 30 ka, was characterized by millennial-scale climate oscillations commonly referred to as Dansgaard-Oeschger (D-O) events. These events, particularly well-defined in Greenland ice cores, were first described by Dansgaard et al. (1993). Typically, D-O events are featured by an abrupt transition (within a few decades) from a cold phase (GS), into a warm phase (GI). NGRIP, GRIP and GISP2 ice cores provide master records for these rapid climatic changes throughout the Last Glacial cycle (MIS 5d to the end of MIS 2; ca. 116–11.7 ka) in the North Atlantic region (McManus et al., 1999). Boundaries between GS and GI periods were established based on both stable-oxygen isotope ratios of the ice ($\delta^{18}O$, reflecting mainly local temperature) and calcium ion concentrations ($[Ca^{2+}]$ reflecting mainly atmospheric dust loading) measured in the ice (**Fig. 1, a-c**) (Rasmussen et al., 2014). The close timing of $\delta^{18}O$ and $[Ca^{2+}]$ abrupt shifts is also indicative of reorganizations in atmospheric circulation (Steffensen et al., 2008). Notably, $[Ca^{2+}]$ data reflect primarily changes in dust concentration but also changes in dust source conditions and transport paths (Fischer et al., 2007a, 2007b). During D-O events North Atlantic region temperature and East Asian storminess were tightly coupled and changed synchronously with no systematic lead or lag (Ruth et al., 2007), thus providing instantaneous climatic feedback. This relationship was stable over the entire Last Glacial period.

According to Petersen et al. (2013), the driving mechanism of GI onset is linked to the rapid collapse of an ice-shelf fringing Greenland, potentially due to subsurface warming.

134   During GI, a gradual cooling controlled by the timing of ice-shelf regrowth leads to GS

135   conditions that lasted for centuries up to millennia. NGRIP temperature reconstructions

136   based on δ^{15}N isotope measurements (**Fig. 1, b**) show T increase at the onset of each GI

137   ranging from 6.5 °C (D-O 9) up to 16.5 °C (D-O 11), with an uncertainty of ±3 °C (Kindler

138   et al., 2014).

139   A recent important step forward is represented by the development of the ice-core GICC05

140   chronology (Andersen et al., 2006; Rasmussen et al., 2006; Svensson et al., 2008;

141   Seierstad et al., 2014) and its flow model-based extension (GICC05modelext) published in

142   Rasmussen et al. (2014), which allowed to achieve a reference template for the pattern of

143   climate variability during the Last Glacial cycle.

144   **2.2   Climate signals in mid- to low-latitude marine records**

145   A well-known feature in North Atlantic marine sediments is the presence of coarse

146   sediment layers, i.e. the ice-rafted debris (IRD, Ruddiman, 1977). Such depositional

147   episodes, known as Heinrich Events (HE), are related to massive discharge, rafting and

148   melting of icebergs into the ocean and the consequent fall of detrital sediments trapped in

149   the ice on the ocean floor (Heinrich, 1988) and unambiguously identified during GS phases

150   of the Last Glacial period (e.g. Bond et al., 1992; 1993; Hemming 2004).

151   It is widely assumed that D-O events and HE are linked to reorganisations and/or

152   variations in the strength of the Atlantic Meridional Overturning Circulation (AMOC)

153   (Broecker et al., 1990). Specifically, Bagniewski et al. (2017) suggest a 30-50% weakening

154   of the AMOC during GSs and a complete shutdown during HEs, also coinciding with large

155   increases in the abundance of foraminifer polar species (e.g. *N. pachyderma*, **Fig. 1, h-g**).

7

156 The Iberian Margin (**Fig.1**) is a key area for the reconstruction of these dynamics thanks to

157 its distal position, i.e. outside of the main belt of ice rafting, which limit disturbance of the

158 sediments (Bard et al., 2000; Pailler and Bard, 2002). The recently obtained Sea Surface

159 Temperature (SST) curve based on the biomarker TEX^{H}_{86} in MD95-2042 core (Darfeuill et

160 al., 2016) highlights that the greater cooling peaks occurred during HEs (about 3-5 °C; **Fig.**

161 **1, f**). This feature is in disagreement with the general pattern emerging over Greenland,

162 where temperatures reconstructed during GS are roughly comparable and show more

163 stable values to each other (**Fig. 1, b**). In addition, Martrat et al. (2007) argue that SST

164 changes occur a few centuries before the subsequent generation of icebergs, which are

165 traced by increases in IRD percentage. Regarding this issue, various studies state that

166 HEs are shorter (Roche et al., 2004; Peters et al., 2008) than the corresponding GS and

167 occur after the AMOC entered a weakening trend (Flückiger et al., 2006; Marcott et al.,

168 2011). Thus, HEs seem to be a consequence rather than the cause of the AMOC

169 weakening (e.g., Alvarez-Solas et al., 2010, 2013; Marcott et al., 2011; Barker et al.,

170 2015).

171 Given the uncertainty across the North Atlantic in the ocean reservoir correction (e.g.,

172 Stern and Lisiecki, 2013; Butzin et al., 2017), and the lack of a clear HE signature in the

173 $\delta^{18}O$ Greenland isotopic record (Rasmussen et al., 2014), it is difficult to establish where

174 HEs lie exactly within the D-O framework (Andrews and Voelker, 2018). Indeed,

175 Rasmussen et al. (2014) did not designate the temporal positions of HEs. However, new

176 Greenland ice cores proxy records (e.g., ^{17}O-excess; **Fig. 1, d**) are linked to a lower-

177 latitude hydrological cycle signal (Guillevic et al., 2014). This might help in the future to

178 better constrain HE in the ice core series, allow exploring time leads and lags in between

179 events happening at different latitudes.

180

181 2.3 Synchronicity between abrupt Greenland events and terrestrial responses in
182 Southern Europe

183 Over the last two decades, the INTIMATE project (INTegrating Ice-core, MArine, and

184 TErrestrial records; e.g., Blockley et al., 2012; Rasmussen et al., 2014) has proposed a

185 series of event-stratigraphic templates based on the isotopic and dust concentration

186 changes in Greenland ice cores. The alternating pattern of stadial and interstadial

187 geologic-climatic units, due to their very high stratigraphic and temporal resolution and

188 precise dating, constitute the most comprehensive and best resolved archive of high-

189 frequency climate variability. The Northern-Hemisphere transmission of such millennial-

190 scale signals (reflected in $\delta^{18}O$ variations) depends on the extremely rapid atmospheric

191 circulation changes (probable lag a couple of years only; Rasmussen et al., 2014). These

192 changes are induced by migration of the Polar Front (PF) and shifts of the Intertropical

193 Convergence Zone (ITCZ) at mid-to-low-latitudes (Europe and the Mediterranean areas)

194 (e.g., Peterson and Haug, 2006), which in turn induce atmospheric circulation and local

195 rainfall changes.

196 Problems in synchronization of MIS 3 records mainly arise from the uncertainties of the

197 age models, based on different dating methods, the intrinsic difficulties in dating these

198 events, in particular for those intervals at or beyond the limit of the radiocarbon technique

199 (see section 7.1) and the scarcity of precisely dated and unambiguously synchronous

9

200 stratigraphic events, such as tephra layers, magnetic excursions and cosmogenic nuclide

201 peaks. Speleothems are excellent archives for recording these abrupt isotopic changes

202 (e.g., Fleitmann et al., 2009; Moseley et al. 2014; Weber et al., 2018), since they are

203 among the most accurately datable archives, i.e., within the last ca 100 ka, two sigma

204 (95%) errors can be below 1% of the U/Th age. Their deposition is predominantly

205 influenced by either temperature (higher latitude) or precipitation (lower latitude), but both

206 ultimately linked to Northern Hemisphere temperature fluctuations (e.g., McDermott, 2004;

207 Genty et al., 2006). In general, speleothem records unambiguously show the signature of

208 D-O cycles and HEs on European and Mediterranean climate, and a millennial to sub-

209 millennial scale synchronicity in climatic shifts between European and Greenland isotopic

210 records. Despite a generally continuous calcite deposition during the GI 14-GI 13 interval,

211 even at the elevation of the modern snowline in the Alps (Spötl and Mangini, 2007;

212 Moseley et al., 2014), their registration is often fragmentary and hiatuses may have

213 occurred during cold/dry phases (i.e. HE 5 and HE 4; Spötl et al., 2002; Moseley e al.

214 2014, **Fig. 1, e;** Weber et al., 2018). In fact, ITCZ variations may have also affected local

215 rainfall patterns, triggering enhanced dryness notably in the Mediterranean (Fletcher and

216 Sánchez Goñi et al., 2008; Fleitmann et al., 2009). However, precise determination of the

217 durations of these hiatuses may provide valuable information about climatic thresholds that

218 affect regional climatic conditions (Moreno et al., 2010; Zhornyak et al., 2011; Stoll et al.,

219 2013). Overall, the climatic pattern underlying these $\delta^{18}O$ profiles during MIS 3 strongly

220 resembles that of Greenland ice cores at millennial scales, and in many cases

221 corresponding to the detail of decadal-scale cooling events within interstadials (Moseley et

222 al., 2014).

3 Reference mid-to-high resolution MIS 3 palaeoecological records in Southern Europe and in the Mediterranean region

Palaeoecological and palaeoclimate archives considered in this review paper (**Tab. 1**) are mostly located in Southern Europe and in the Mediterranean region between ca. 36° and 46.5° N throughout the Atlantic, Continental, Alpine, and Mediterranean biogeographical regions (**Fig. 2**; European Environment Agency, 2016). A few others dataset from central Europe accompany these sites. Selected records (i) cover a relevant interval during the ca. 30 – 60 ka time-frame, (ii) are mostly characterized by a sub-millennial/multi-decadal time resolution (see **Tab. 1**), and (iii) include quantitative or semi-quantitative geochemical (i.e., stable isotopes) and/or vegetation (i.e. palynological data) climate proxy variables. Most of them are placed in the Mediterranean region, which borders the Atlantic region in the west and the western Eurasian sub-continental region including both the Black Sea and the Anatolian regions (**Fig. 2**). The latter area is of particular interest because it possibly served as a gateway for the spread of AMHs into Europe (Müller et al., 2011). Thus, palaeoclimatic and palaeoecological information from these sites are of great importance and serve as background for the archaeological work in the Levant.

239

Site	Archive type	Latitude (decimal degrees)	Longitude (decimal degrees)	Elevation (m asl)	Interval/Time period (ka)	Palaeoenvironmental /climate proxies	Mean temporal resolution for MIS 3 (yrs/sample)	References
TERRESTRIAL								
Abric Romani (Spain)	Carbonate sediments/ travertine deposits	41.53	1.68	310	41-70 ka	Palynological data	200 yrs	*Burjachs et al., 2012*
Azzano Decimo (Italy)	Lake sediments	45.85	12.9	10	0-215 ka (discontinuous)	Palynological data	1150 yrs	*Pini et al., 2009*
Lac du Bouchet (France)	Lake sediments	44.83	3.82	1200	ca. 8-120 ka	Palynological data	ca. 1000 yrs	*Reille and Beaulieu, 1990*
Eifel maar (Germany)	Lake sediments	50.16	6.85	420	0-60 ka	Palynological data	Decadal/centennial	*Sirocko et al., 2016*
Fimon (Italy)	Lake sediments	45.46	11.53	23	27-138 ka	Palynological data	960 yrs	*Pini et al., 2010*
Füramoos (Germany)	Peat deposits	47.98	9.88	662	0-14 ka, 40-140 ka	Palynological data	ca. 900-1200 yrs	*Müller et al., 2003*
Ioannina 284 (Greece)	Lake sediments	39.75	20.85	470	0-132 ka	Palynological data	325 yrs	*Tzedakis et al., 2002*
La Grand Pile (France)	Lake sediments	47.73	6.50	330	0-140 ka	Palynological data	ca. 250 yrs	*Woillard 1978; Guiot et al., 1992*

Lagaccione (Italy)	Lake sediments	42.57	11.8	355	4-100 ka	Palynological data	420 yrs	*Magri, 1999*
Les Echets (France)	Lake sediments	45.9	4.93	267	ca. 10-75 ka	Palynological data	ca. 500 yrs	*Beaulieu and Reille, 1984*
Kopais K-93 (Greece)	Lake sediments	38.43	23.05	95	10-130 ka	Palynological data	830 yrs	*Tzedakis, 1999*
Megali Limni (Greece)	Lake sediments	39.1	26.32	323	22-62 ka	Palynological data	150 yrs	*Margari et al., 2009*
Lago Grande di Monticchio (Italy)	Lake sediments	40.93	15.62	656	0-132 ka	Palynological data	210 yrs	*Allen et al. 1999; Wutke et al., 2015*
Ohrid (Republic of Macedonia and Albania)	Lake sediments	40.91	20.67	693	0-500 ka	Palynological data	ca. 850 yrs	*Sadori et al. 2016*
Prespa (Republic of Macedonia, Albania and Greece)	Lake sediments	40.95	20.96	849	0-92 ka	Palynological data	ca. 1070 yrs	*Panagiotopoulos et al. 2014*
Ribains (France)	Lake sediments	44.83	3.82	1075	10-150 ka	Palynological data	ca. 1500 yrs	*Beaulieu and Reille, 1992b*
Tenaghi Phillippon (TF II) (Greece)	Peat-dominated succession	41.17	24.33	40	0-130 ka	Palynological data	120 yrs	*Wijmstra 1969; Müller et al., 2011; Wulf et al., 2018*

13

Valle di Castiglione (Italy)	Lake sediments	41.88	12.77	44	0-250 ka	Palynological data	440 yrs	*Follieri et al., 1988-1998*
Lago di Vico (Italy)	Lake sediments	42.32	12.28	507	0-90 ka	Palynological data	ca. 500 yrs	*Leroy et al., 1996; Magri and Sadori, 1999.*
Bunker cave - Bu2 (Germany)	Speleothems	51.36	7.6	184	From 52 to 50.9 ka and from 47.3 to 42.8 ka	Calcite δ^{18}O, δ^{13}C	decadal/ multidecadal-scale	*Weber et al., 2018*
Hölloch cave (Höl-7, Höl-16, Höl-17, and Höl-18) - NALSP (Germany)	Speleothems	47.38	10.15	1240–1438	35-65 ka (discontinuous)	Calcite δ^{18}O, δ^{13}C	decadal/ multidecadal-scale	*Mosely et al., 2014*
Kleegruben cave - SPA 49 (Austria)	Speleothems	47.09	11.67	2165	46-58 ka	Calcite δ^{18}O, δ^{13}C	decadal/ multidecadal-scale	*Spötl et al., 2002*
Soreq cave (Israel)	Speleothems	31.7	35	400	0-60 ka	Calcite δ^{18}O, δ^{13}C	40 yrs	*Bar-Matthews et al., 1999-2000*
Villars cave - Vil 27 (France)	Speleothems	45.3	0.5	175	30-55 ka	Calcite δ^{18}O, δ^{13}C)	53 yrs (between 48.5 and 40.5 ka) and 203 yrs (between 40.5 and 30 ka)	*Genty et al., 2010*

14

Villars cave - Vil 9 (France)	Speleothems	45.3	0.5	175	32-83 ka (discontinuous)	Calcite δ^{18}O, δ^{13}C	91 yrs (between 51.8 and 40.4 ka) and 195 yrs (between 40.4 and 31.8 ka)	*Genty et al., 2003*
Villars cave - Vil 14 (France)	Speleothems	45.3	0.5	175	29-52 ka	Calcite δ^{18}O, δ^{13}C	81 yrs (between 52.2 and 41.7 ka) and 1066 yrs (between 41.7 and 28.9 ka)	*Wainer et al., 2009*
NGRIP (Greenland)	Ice core	75.1	42.32	2917	8-120 ka	δ^{18}O; calcium ion concentration data ([Ca2+])	re-sampled to 20-year resolution	*Seierstad et al., 2014; Rasmussen et al., 2014*
MARINE								
MD04-2845 (Western France)	Marine sediments	45.35	-5.22	-4100	30-140 ka	Palynological data; Foraminiferal δ^{18}O; Ice-rafted debris record	540 yrs	*Sánchez Goñi et al., 2008*
MD95-2042 (Iberian margin)	Marine sediments	37.8	-10.17	-3148	27-138 ka	Palynological data; Foraminiferal δ^{18}O; Ice-rafted debris record; $U^{k'}_{37}$ and TEX_{86} biomarkers (SST)	ca. 370 yrs	*Sánchez Goñi et al., 1999-2000-2008-2009*

15

MD95-2043 (Alboran sea)	Marine sediments	36.13	-2.62	-1841	0-50 ka	Palynological data; Foraminiferal δ^{18}O; C_{37} Alchenones (SST)	260 yrs	*Cacho et al., 1999; Sánchez Goñi et al., 1999; Fletcher and Sánchez Goñi, 2008*
LC21 (Aegean sea)	Marine sediments	35.66	26.58	-1522	0-160 ka	Foraminiferal δ^{18}O	ca. 200 yrs	*Grant et al., 2012*
ODP 976 (Alboran sea)	Marine sediments	36.20	-4.30	-1108	>1Ma	Palynological data; Foraminiferal δ^{18}O	Ranging between 50 and 200 yrs	*Combourieu-Nebout et al., 2002; Combourieu-Nebout et al., 2009; Genty et al., 2010*

240

241 **Tab. 1** List of selected sites from S-Europe and the Mediterranean area that entirely or partially cover the MIS 3 chronological framework,
242 specifying location, available vegetation-climate proxy variables and time resolution. References to published data are also indicated

243

3.1 Vegetation response to D-O events and HEs in Southern Europe and Mediterranean region

The history of vegetation during MIS 3 in Southern Europe and in the Mediterranean area relies on several palaeoecological studies carried out in lake and peat stratigraphic sequences. In **Fig. 3** we consider the evidence for millennial-scale variability and long-term vegetation trends from selected records covering the period between ca. 60 - 30 ka (i.e., GI 17 to GI 5). The records are presented on the most recent chronology available for each one. On the whole, this data shows a high sensitivity of vegetation response to D-O events, making South Eastern Europe and the Italian Peninsula a key geographical area for high-resolution palaeoenvironmental researches during the last glacial period.

In southern Europe, the recurrent succession of (open) woodlands, including temperate taxa, and grasslands with xerophytic elements (**Fig. 3**), have been tentatively correlated to GIs in Greenland ice cores (Fletcher et al., 2010b). This assumption is reasonable for this geographic area as thermophilous trees persisted in refugia and appeared to have expanded rapidly during each interstadial without substantial migration lags (Harrison and Sánchez Goñi, 2010).

Investigations at Lago Grande di Monticchio (Allen et al., 1999, 2000) were the first to provide an independently dated Late Pleistocene palaeoenvironmental record, due to its varved sequence. Furthermore, the identification of known tephra layers, one of which is the Campanian Ignimbrite (CI), has also been used to improve the age-depth model (Wutke et al., 2015). The high-resolution pollen record (ca. 200 yrs/sample) obtained from

17

265   the Monticchio core reveals millennial-scale changes in woody/open environments

266   throughout MIS 3. Palaeoecological data indicate an alternation between cold/dry steppic

267   vegetation, referred to GS periods, and an increased range of woody taxa including

268   deciduous *Quercus*, *Abies* and *Fagus* (up to 30–60% AP), referred to GI periods (Allen et

269   al., 1999; Fletcher et al., 2010b). Similarly, other long pollen records from volcanic lakes in

270   central and southern Italy, i.e., Lagaccione and Valle di Castiglione (**Fig. 3**; Follieri et al.,

271   1988, 1998; Magri, 1999), show remarkable changes of vegetation composition, structure

272   and biomass including millennial-scale fluctuations in forest development with deciduous

273   and evergreen *Quercus, Corylus, Fagus*, *Betula* and *Picea* (Fletcher et al., 2010b). The

274   lower temporal resolution of these latter records (ca. 400 yr/sample) in turn reduced the

275   chances to precisely identify each GI (**Fig. 3**).

276   In northern Italy, pollen records from Lake Fimon (**Fig. 3**) and Azzano Decimo (Pini et al.,

277   2009; Pini et al., 2010) indicate phases of conifer-dominated forest expansion (*Pinus*

278   *sylvestris-mugo* and *Picea*), rich in cool broad-leaved trees (*Alnus* cf*. incana* and tree

279   *Betula*) and accompanied by a reduced warm-temperate component (*Tilia*). In both

280   records, individual D–O events cannot be identified due to the low temporal resolution (ca.

281   800-1000 yr/sample), nevertheless the well-documented long vegetation trend is indicative

282   of a persistent afforestation. In fact, only moderate forest withdrawals occurred and some

283   temperate trees (e.g., *Tilia* and *Abies*) persisted up to ca. 40 ka BP (Pini et al., 2010).

284   Interestingly, peaks of *Tilia* pollen were found (Cattani and Renault-Miskowski, 1983-84) in

285   layers preserving Mousterian artefacts and dated to 40.6-46.4 ^{14}C ka in the cave

286   sediments at the Broion shelter (Leonardi and Broglio, 1966), and also in Paina cave inter-

287   pleniglacial deposits (Bartolomei et al., 1987-88; Cattani 1990).

18

288   At southern latitudes, high-resolution pollen records from Ioannina, Tenaghi Philippon and

289   Megali Limni (Greece, **Fig. 2** and **Fig. 3;** Wijmstra, 1969; Tzedakis et al., 2006; Margari et

290   al., 2009; Müller et al., 2011; Wulf et al., 2018,) show exceptional series of millennial and

291   sub-millennial vegetation changes correlated to a number of GI/GS (Fletcher et al. 2010b;

292   Pross et al. 2015). Concerning colder phases, the GSs related to HEs appear to have a

293   more pronounced effect than other GSs on woodland withdrawal and xerophytes

294   expansion. Notably, GS 9-HE 4 phase corresponds to the most severe reduction of tree

295   cover in a number of records (e.g., Megali Limni, Tenaghi Philippon, Valle di Castiglione

296   and Ioannina; **Fig. 3**). Interestingly, pollen records from different bioclimatic areas seem to

297   show differences in terms of magnitude of the response to cold events due to local

298   ecosystem structures. In sites where moisture availability was not a limiting factor,

299   differences in the magnitude of climate forcing during HEs seem to be well expressed in

300   terms of major vegetation changes (e.g., Ioannina, Monticchio) (**Fig. 3**). However, where

301   temperate tree populations were near their tolerance limit, the environmental stress

302   associated with HEs probably crossed a critical threshold resulting in large population

303   contraction with an almost complete drop in forest cover (i.e., Tenaghi Philippon, Megali

304   Limni) (Tzedakis et al., 2004) (**Fig. 3**).

305   On a long-term scale, a reduction/opening of forests throughout MIS 3 (see **Fig. 3**) took

306   place from GI 14, showing a maximum in woodland density, to the following GI 12 and GI

307   8. During GI 14/ 13 interval, conditions were notably humid and mild in the eastern

308   Mediterranean as indicated by the Soreq cave isotopic record (Bar-Matthews et al., 2000)

309   and also over Europe (Allen et al.,1999; Sánchez Goñi et al., 2002; Fletcher et al., 2010b).

310   Despite the relatively high amount of palaeoecological information for southern Europe,

311   the spatial distribution of records in this heterogeneous geographic sector remains uneven.

312   Such differences in the expression of millennial-scale events suggest that site

313   characteristics need to be taken into account when mapping the spatial patterns of

314   changes and trying to elucidate the mechanisms involved. New records are needed (e.g.,

315   from northern and southern Italy, Turkey, the Levant), in order to refine the knowledge of

316   eco-climatic gradients across the continent and to better understand regional vegetation

317   patterns.

318   **3.2   Fire dynamics in Southern Europe and Mediterranean region**

319   High-resolution microcharcoal records can provide new insights to understand fire-

320   vegetation dynamics in relation to climate variability (e.g. D-O cyclicity/HE events) and/or

321   human activities (e.g., Whitlock and Larsen, 2001; Iglesias et al., 2015). As for the Last

322   Glacial period, few microcharcoal records are available from terrestrial (e.g., Magri, 2008;

323   Margari et al., 2009; Pini et al., 2009, 2010) and marine records (e.g., Daniau et al., 2007,

324   2009). **Fig. 3** shows microcharcoal data for some Southern East European terrestrial sites:

325   Lake Fimon, Valle di Castiglione, Lagaccione and Megali Limni (MIS 3 partially

326   documented).

327   Overall, a fire regime variability mainly associated with fluctuations in forest cover occurred

328   between GS (lower fire activity) and GI (higher fire activity). Higher microcharcoal

329   concentration during periods of afforestation suggests enhanced fire activity favoured by

330   increasing woody fuel and biomass accumulation during GI (Magri, 1994), as observed

331   also by Daniau et al. (2007; 2009) for southwestern Iberia (MD95-2042 and MD04-2845

332   cores, **Fig. 2**). Contrary to this pattern, NE-Italy experienced isolated major fire episodes

20

333 over a generally low-intensity fire regime; at Lake Fimon (Pini et al., 2010; **Fig. 2**) the

334 strongest fire episode of the whole Late Pleistocene record is coeval to a drop in forest

335 cover mirrored by steppe expansion, possibly correlated to HE4 (**Fig. 3**). Since the

336 palaeoecological data from this site suggest relatively high moisture availability during MIS

337 3 (Pini et al., 2010), such climatic context may have prevented long-term fire activity south

338 of the Alps, despite biomass availability. This evidence indicates that the incidence of fires

339 is not always directly correlated with the degree of afforestation. This framework supports

340 a regional climatic influence on fire regimes over SE-Europe with a direct climatic control

341 on fuel availability during the Last Glacial period.

342

343 **4 Snapshots of European palaeogeography and ecoclimatic zones**
344   **during GI 12 and the LGM**

345 With the aim of setting Palaeolithic humans in a palaeoenvironmental scenario, we chose

346 two MIS 3-2 key intervals relevant for the human evolution and marking paleoclimate

347 extreme conditions: the GI 12 and LGM. We plotted the main European palaeogeography

348 and palaeoecology landscape features on geographical snapshots (**Figure 4A and B**). In

349 detail, GI 12 snapshot (ca. 46.8 to 44.2 ka according to Rassmussen et al., 2014)

350 represents a phase of major forest expansion during MIS 3 also coincident with the AMHs

351 arrival in Europe (Grotta del Cavallo, ca. 45.5 ka; Benazzi et al., 2011; Zanchetta et al.,

352 2018) (**Figure 4A).** The second one spans the time interval of both the SIS (Scandinavian

353 Ice Sheet) and the European mountain glacier culminations during the LGM (26 to 21 ka

354 cal BP in Europe, see Hughes et al., 2016; Monegato et al., 2017), which was

355 characterized by one of the most pronounced forest contractions of MIS 3-2 time span

21

356 (**Figure 4B**). From GI 12 to LGM, climate changes led to dramatic variations in glacier

357 extent and sea level with major impacts on the physiography of mountain areas, coastal

358 regions and the hydrologic systems. The latter two are also known for their important role

359 in AMHs dispersal into Europe (Mellars, 2006; Hublin, 2014).

4.1   Palaeoenvironmental setting during Greenland Interstadial 12 (MIS 3)

4.1.1. Reconstructed gradients ecogeography within eco-climatic zones

362 We reconstructed terrestrial ecosystems for a time frame corresponding to GI 12 (**Fig. 4A**)

363 by combining palaeobotanical records (for Central Europe: see Van Meerbeeck et al.,

364 2011 and references therein; Follieri et al., 1988; Beaulieu and Reille, 1992a-b; Drescher-

365 Schneider et al., 2007; for Mediterranean Europe: Magri, 1999; Sánchez Goñi et al., 2002

366 and 2009; Pini et al., 2009, 2010; Müller et al., 2011) and ecoclimatic gradients. These

367 gradients rely both on large scale latitudinal zones (i.e., Tundra zone and Forest-tundra

368 zone, and related positions of polar timberline, see Holtmeier,1985; Archibold, 2012),

369 spanning the northern half of European subcontinent and on regional elevational mountain

370 belts in southern Europe (see Fig. 4A). We assumed GI 12 and GI 14 vegetation peaks to

371 have been similar at the same site, although GI 12 was shorter, and used both GI 14 and

372 GI 12 data to implement our reference dataset. Fossil data was improved by (a)

373 elevational ecoclimatic relationships and (b) vegetation models (Alfano et al., 2003).

374 However, available gridded vegetation models do not account for vegetation distribution in

375 complex mountain regions that actually represent 75% (total areas above 500 m altitude

376 obtained from GIS elaboration) of the southern European landscape. Indeed, elevation

377 gradients can be very steep and, within a 1-km^2 grid cell, elevation can vary up to, or even

378 more than, 500 m. In these contexts, forests display a characteristic discontinuity in their

379 distribution with a main boundary representing the upper limit of forest canopies

380 associated with temperature decrease along elevational gradients. Thus, some

381 inaccuracies in the vegetation distribution can be expected in global models due to the

382 coarse spatial resolution of climate datasets that can be affected by errors in the local

383 temperature estimation (i.e., more than 1°C for a lapse rate of about −0.5°C/100 m).

384 A number of ecoclimatic zones are featured by distinct regional climates (i.e. coniferous

385 and broad-leaved woodlands along the northern coast of Portugal and Spain; map of the

386 European Environment Agency, 2015). Within each zone, local climates (i.e. mountain

387 areas) have been qualified by elevational gradients of orographic precipitation. The main

388 features of these altitudinal gradients are the upper timberline limit and the glacier

389 Equilibrium Line Altitude. Given the determinants of the warmest month temperature

390 (TJuly) on the upper timberline, caused by heat deficiency (Tranquillini, 1979; Jobbagy and

391 Jackson, 2000; Körner and Paulsen, 2004), we used TJuly reconstructions for GI 12 to

392 estimate the altitude of montane timberline. In order to moderate the effects of CO_2

393 changes on plant fertilization (Farquhar, 1997), we included past timberlines as calibration

394 test of our estimations. The timberline position in the Italian Central Alps during the

395 Bølling-Allerød (1700-1800 m asl: Tinner et al., 1999; Ravazzi et al., 2007) is a good test

396 as the GI 1 is the only D-O interstadial which occurred under moderately low CO_2

397 concentration; furthermore, relevant fossil records are relatively common as they were not

398 erased by LGM glacier activity. Given the position of the alpine timberline during the

399 Bølling-Allerød and the associated pollen-based mean TJuly (18,5-19°C; Vallè et al.,

400 unpublished data), we infer the timberline position during GI12 using the difference

401 between TJuly for GI12 (ca. 18°C) and the Bølling-Allerød. This difference was projected

402 over an elevational gradient using an average environmental lapse rate of about -

403 0,67°C/100 m (Furlanetto et al., 2019), to obtain an historical timberline for GI 12 (ca. 1600

404 m in the Italian Central Alps). The method was also tentatively applied to estimate

405 timberlines in the Mediterranean region. Here, however, many boreal tree species were

406 missing during MIS 3, thus ecophysiological requirements of Mediterranean timberline

407 species were considered.

408 **4.1.2. Estimating Equilibrium Line Altitudes of mountain glaciers**

409 By using elevational lapse rates we also estimated the Equilibrium Line Altitude (ELA)

410 position during GI12 in the Central Alps (Vallé et al., unpublished data). Again,

411 temperature differences between the LGM ELA positions (e.g. Kuhlemann et al. 2008;

412 Hughes and Woodward, 2016) and GI 12 were projected over elevational gradients and

413 tested against the temperatures and ELA related to the Egesen stage, Younger Dryas

414 (Kelly et al., 2004; Ivy-Ochs et al., 2008; Delmas, 2015; Ruszkiczay-Rüdiger et al., 2016;

415 Popescu et al., 2017; Gromig et al., 2018). The results of a recent Parallel Ice Sheet Model

416 (PISM) with climate forcing deriving from WorldClim and the ERA-Interim reanalysis

417 (Seguinot et al., 2018) proved to fit our results for the Central Alps (GI 12 ELA 2100 m,

418 626 m higher than the LGM ELA). As a best approximation, the same value was added to

419 the LGM ELA position for the Pyrenees, Balkans and Carpathians, providing a GI12

420 reconstructed ELA of ca. 2400 m, ca. 2100 m and 2000 m, respectively.

421 **4.1.3. The GI 12 palaeoenvironmental map**

422 European vegetation gradients were particularly strong during the major interstadial

423 phases (i.e., spanning about 2000-2500 years), characterized by large arboreal excursions

424   both latitudinally and altitudinally, north and south of the Alps. The GI 12 is one of these

425   key representative warm intervals. In **Figure 4A,** we depict the palaeoenvironmental

426   setting of mid and southern Europe (between 52° and 35° latitude N) during GI 12. It is

427   also shown a reconstruction of the coastline: -74 m a.s.l. (Waelbroeck et al., 2002;

428   Antonioli, 2012). A substantial seashore enlargement over Europe led to increased

429   connectivity, especially between the Italian peninsula and the Western Balkans region,

430   between Mediterranean islands, and also the emergence of large areas north of the Black

431   Sea and in the North Sea (**Fig. 4A**). The Scandinavian Ice Sheet (SIS), which grew during

432   MIS 4, had almost entirely melted at mid MIS 3 (60–45 ka) (Lambeck et al., 2010;

433   Wohlfarth, 2010).

434   We summarize hereafter the main constrains of the featured ecoclimatic zones.

435   **Forest tundra ecozone**. The northern timberline was given as the northern limit of the

436   forest tundra mosaic (*sensu* Walter and Breckle, 1986; Holtmeier, 2009; Van Meerbeeck et

437   al., 2011). The abundance of gleysols with charred wood dated to around 45 ka at the

438   base of loess-luvisol sequences in Central and Eastern Europe (Haesaerts et al., 2009;

439   Moine et al., 2017) supports locating the zonoecotone of forest tundra for wetter

440   interstadial phases of MIS 3 between 47° and 52° - 54° N, i.e. north of the Alps (Fig. 2A).

441   The geography of northern timberline in Central and Eastern Europe was drawn according

442   to modelling results by Alfano et al. (2003). In the forest tundra zonoecotone, the forest is

443   found mainly in warmer and drier places, with stunted individuals at the waterlogging

444   edaphic ecotone.

25

445 **Atlantic zone.** This biogeographical region closely interacts with the northeast Atlantic

446 Ocean margin. Expansion of Atlantic forests with *Betula, Pinus* and deciduous *Quercus* is

447 recorded during GI 12 and 14, probably reflecting obliquity forcing at higher latitudes

448 (Sánchez Goñi et al., 2008). Vegetation in Western Iberia also responded immediately

449 (within the resolution of the record) to SST changes on millennial time scales during MIS 3.

450 Increases in temperatures offshore translated to increased tree cover on land and vice

451 versa. This rapid response to interstadials warming supports the idea that thermophilous

452 taxa persisted in NW-Iberian refugia throughout the last glacial period (Roucoux et al.,

453 2005).

454 **Iberian region.** Average annual precipitation map for the Iberian peninsula (years 1901-

455 2009; Schneider et al., 2014) depicts a strong gradient from the north-western to northern

456 Atlantic coasts (1100 - 1500 mm/year) to central Spain and Mediterranean areas (250 -

457 700 mm/year). During GI 12, humid Atlantic air masses promoted higher moisture

458 availability on the northern coasts of Portugal and Spain, which could support the

459 occurrence of open temperate woodlands. In the inner Iberian areas, grasslands occupied

460 drier lowlands; increasing afforestation was visible along altitudinal gradients.

461 **Adriatic and Tyrrhenian Basins.** Lowering of the sea led to the emergence of a wide

462 area north of the 44° parallel in the Adriatic sea. The area hosted terrestrial vegetation,

463 from mixed conifer and broad-leaved woodlands in the inner Friulian-Venetian Plain to

464 more open communities and then grasslands, the latter building a wide belt along the

465 coastal margins. Differences in the humidity regimes between the eastern Adriatic and the

466 western Tyrrhenian Basins bordering Italy are responsible for the asymmetry of

26

467 ecosystems represented in Fig. 2A. Palaeoecological records from the Tyrrhenian coast

468 suggest almost persistent moisture availability during MIS 3. Similar to the current

469 situation, it can be assumed that precipitation was mainly generated by the orographic

470 uplift of air charged with moisture from the Tyrrhenian Sea.

471 **Balkans and Aegean regions:** During GI 12, terrestrial ecosystems were dominated by

472 open temperate woodland and/or temperate forest-steppe south of 40°N, with increasing

473 amount of trees north of this latitude. At lower altitudes, in wider belts bordering the

474 eastern Adriatic, Ionian and eastern Mediterranean Seas, grasslands developed.

475 **Central Anatolian plateau.** In the Anatolian region the reconstructed historical GI 12

476 timberline is located at 1500 m asl. Areas down to 500-800 m could support open forest

477 vegetation, especially along the Turkish coasts of the Black Sea, characterized by a

478 temperate oceanic climate with the greatest amount of precipitation of the whole region

479 (Turkish State Meteorological Service, 2006). Moisture does not reach inland areas; inner

480 plateau bordered by the Pontic Mountains to the north and the Taurus to the south is

481 characterized by a continental climate with strongly contrasting seasons. During GI12, in

482 these inner areas open grasslands expanded.

483 A reconstruction of European vegetation patterns during a warm/moist phase of MIS3 was

484 proposed by van Andel and Tzedakis (1998). The vegetation subdivisions provided in this

485 early reconstruction largely overlap with the picture of terrestrial ecosystems provided in

486 our Fig. 2A, with some differences **(i)** the reconstruction of van Andel and Tzedakis (1998)

487 is plotted on a simplified sketch map of Europe not taking into account the altitudinal

488 gradients, indeed represented on our GIS topographic base. This is important as far as

489 temperature and moisture gradients play an important role in determining both latitudinally

490 and altitudinally extents of vegetation belts; **(ii)** minor differences between the two

491 reconstructions are visible in the shape of the limit of the northern timberline (between 53-

492 55°N in Fig. 2A - based on Alfano et al., 2003; around 50°N according to van Andel and

493 Tzedakis, 1998); **(iii)** Fig. 2A provides indication on ELA and timberline positions during an

494 interstadial, thanks to data from papers published in recent years and quantitative climate

495 reconstructions for the last glacial cycle.

496 **4.2 Palaeogeography of Southern and Central Europe during LGM**

497 We attempted a LGM palaeogeographical reconstruction of mid-southern Europe in order

498 to allow direct comparison of physical patterns between GI 12 (i.e. a major interstadial

499 within MIS 3) and the subsequent LGM (i.e. 30 to 16.5 ka cal BP, Lambeck et al., 2014)

500 cold phase. For this map, we chose to represent the physical geography of Europe during

501 the time interval spanning both the SIS and the European mountain glacier culminations

502 (26 to 21 ka cal BP in Europe, see Hughes et al., 2016; Monegato et al., 2017). At this

503 time, main climatic patterns can be displayed though different climate zones according to

504 Köppen-Geiger classification (Becker et al., 2015).

505 The SIS passed the coast of western Norway at the time of the Laschamp palaeomagnetic

506 excursion (ca. 41 ka) (Valen et al., 1995; Mangerud et al., 2010). At ca. 21 ka the ice-sheet

507 attained its maximum extent (**Fig. 4 B**; Hughes et al., 2016). During this period the

508 European Alps were extensively covered by an ice-dome which generated valley glaciers.

509 In the Alps, the maximum ice extent was reached during the LGM around 25 ka, when

510 large piedmont glaciers advanced onto the Alpine foreland. This is well constrained by the

511 end-moraine systems, in which the LGM moraines were dated (radiocarbon, OSL and

512   cosmogenic nuclide surface exposure dating methods) and point to large ice lobes at the

513   outlet of major valleys (e.g., Monegato et al., 2007, 2017; Ivy-Ochs et al., 2008, 2018;

514   Ravazzi et al., 2012; Reber et al., 2014; Salcher et al., 2015). In the south-western and in

515   the eastern sectors many valley glaciers remained confined within the valley (e.g., Jorda et

516   al., 2000; Bavec and Verbic, 2011; Rossato et al., 2013, 2018; Federici et al., 2016), as

517   testified by the reconstruction of LGM moraines. In the fringe area of the Alpine chain

518   many isolated small ice caps or mountain glaciers developed without merging with the

519   major trunk glaciers (e.g., Carraro and Sauro, 1979; Forno et al., 2010; Monegato, 2012).

520   Large outwash megafans developed from the front of the Alpine glaciers or from the

521   funnelling of outwash streams in the lower reach of the valleys (Fontana et al., 2014). By

522   this time, large glaciers developed in the Pyrenees and many frontal moraines were dated

523   (Delmas, 2015 and references therein); here glaciers mostly remained confined within the

524   valleys and several small and isolated glaciers occurred (e.g., Pallas et al., 2010). Other

525   small glacier systems were present in the Iberian mountains; these advances had different

526   age development, from 31 to 20 ka, according to Oliva et al. (2019) compilation.

527   Documented ice-caps in the French Massif Central (de Gôer, 1972) and in the Vosges

528   (Seret et al., 1990), but chronology on glacial landforms needs to be improved

529   (Buoncristiani and Campy, 2004).

530   Valley glaciers spread in the Carpathians and Tatra ranges (e.g., Ehlers et al., 2011;

531   Makos et al., 2018). Their size were reconstructed on the basis of remote sensing and field

532   analyses (Zasadni and Klapyta, 2014) and the age of their maximum spread is constrained

533   with exposure dating at about 25 ka (Engel et al., 2015; Makos et al., 2018).

534   The Balkan Peninsula was deeply studied in the last decay (see Hughes and Woodward,

535   2016 for a review). Therein, mountain glaciers developed in a karstic environment with

536   specific characteristics (Adamson et al., 2014; Zebre and Stepisnik, 2015; Zebre et al.,

537   2016). Most of the outwash system into the karstic network and the outwash fans were

538   very confined and limited to the basins where glaciers flowed (Zebre et al., 2016, 2019).

539   Also small glaciers formed on the highest mountain chains of the Apennines (e.g., Giraudi

540   and Giaccio, 2016; Baroni et al., 2018; Mariani et al., 2018).

541   The region surrounding the Adriatic lowstand plain collected the drainage from Alpine

542   outwash systems and from the surrounding Apennine and Balkan rivers, which had

543   important karst underground flows. The large Adriatic lowstand delta (**Fig. 4B**; Maselli et

544   al., 2014; Pellegrini et al., 2015) accreted as sea level fell down to -120 m or -149 m

545   (Antonioli and Vai, 2004).

546   Late Pleistocene aeolian sediments are widespread in Europe (e.g. Haase et al., 2007;

547   **Fig. 4B**) and they represent further indicators of past environmental changes. Loess is

548   commonly distributed in Central, Eastern, and Southern Europe (e.g., Kukla, 1975;

549   Smalley and Leach, 1978; Frechen et al., 1997; Haase et al., 2007; Cremaschi et al.,

550   2015; Marković et al., 2015; Terhorst et al., 2015; Zerboni et al., 2018); in the

551   Mediterranean region loess bodies formed also along the present day coastline (Chiesa et

552   al., 1990; Cremaschi, 1990; Wacha et al., 2011a,b; Boretto et al., 2017). Loess is generally

553   associated with glacial environmental conditions, with dry and cool climate and increased

554   wind strength (Pye, 1995). In continental Europe and in the Mediterranean basin

555   Pleistocene loess accumulated in mid-continental plains free of ice sheets, at the margins

556   of mountain ranges, along the shorelines of the Mediterranean and at the semi-arid

557 margins of the Sahara and Levantine deserts (Obruchev, 1914; Cremaschi, 1990; Haase

558 et al., 2007; Crouvi et al., 2010; Lindner et al., 2017; Lehmkuhl et al., 2018 a,b; Zerboni et

559 al., 2018). In Mediterranean Europe, as in the Po Plain, major loess sources are the

560 outwash plains fed by glaciers flowing from mountains (Alps and Apennines)

561 (Cremaschi,1990). Loess deposition occurred during most of the Quaternary glacials and

562 was related to a general decrease in forest cover and expansion of semideserts, steppe,

563 and treeless environments (Rousseau et al., 2018). Notwithstanding many efforts in

564 establishing fine MIS 4 to 2 loess chronology with luminescence methods and stratigraphic

565 correlations (e.g., Timar et al., 2010; Timar-Gabor et al., 2011; Thiel et al., 2014) due to

566 intrinsic properties of loess and to the possible occurrence of sedimentary gaps (Thiel et

567 al., 2014), the resolution of loess studies is still lower than those of other continental

568 archives. Likely, Late Pleistocene loess sedimentation occurred, at least, since the end of

569 MIS4 and during MIS 3 and 2 (Marković et al., 2015; Terhorst et al., 2015). In Italy, loess

570 sedimentation is recorded along the margins of the Po Plain and discontinuously along the

571 shorelines of the Mediterranean, where loess is better preserved within rockshelters

572 (Cremaschi, 2004; Peresani et al., 2008). Italian loess dates back to the Late Pleistocene

573 and mostly formed since the end of MIS 4 (Cremaschi, 1990, 2004); but loess deposits

574 occur as well in sections that contain Mousterian artifacts dating to MIS 3 (e.g., Cremaschi,

575 1990; Cremaschi et al., 2015; Zerboni et al., 2015; Delpiano et al., 2019). More recently, a

576 few loess bodies have been dated also to MIS 2 (Ferraro, 2009; Zerboni et al., 2015),

577 showing a good continuity in wind sedimentation in the Late Pleistocene, at least at the

578 northern margin of the Po Plain. Italian loess is often interlayered by paleosols, allowing

579 the identification of less arid phases. For instance, at the Val Sorda section a chernozem-

580 like palaeosoil, has been dated at ca. 27 ka BP (Ferraro et al., 2009); whereas at Monte

581 Netto site moderate pedogenesis (including clay illuviation) compatible with forest cover

582 occurred at times between 44 and 25 ka BP (Zerboni et al., 2015).

5   Focus on spatial vegetation response in Italy during MIS 3

584 The pie charts presented in **Fig. 5** show long-term vegetation dynamics and geographic

585 patterns in Italy between ca. 30 and 60 ka cal BP using data from privileged sites (North to

586 South): Lake Fimon, Lagaccione, Valle di Castiglione and Monticchio. For each record,

587 selected pollen taxa are consistently grouped according to their ecology and climate

588 preferences in order to facilitate their comparison (for further information see caption and

589 legend in **Fig. 5**).

590 A higher forest cover in Northern Italy compared to Mediterranean sites is an unchanged

591 background feature during MIS 3. Indeed, the glaciated Alps must have represented a very

592 sharp rainfall boundary leading to more humid conditions in south-eastern alpine foreland

593 persistently forested and a northern treeless boreal and continental landscape, as shown

594 by La Grande Pile, Les Echets and Füramoos pollen records (**Fig. 2**; Woillard, 1978;

595 Beaulieu and Reille, 1984; Guiot et al., 1992; Müller et al., 2003). The palaeoecological

596 record from Lake Fimon documents a mosaic of boreal forests dominated by *Pinus*

597 *sylvestris/mugo* over the 60 to 30 ka cal BP time period. However, a continuous xerophytic

598 steppe expansion (e.g. *Artemisia* and Chenopodiaceae), coupled with the reduction of

599 temperate elements (deciduous *Quercus* and other thermophilous taxa) in favour of pine

600 woodlands, notably since 40-45 ka, suggests a shift towards drier/colder conditions

601 possibly enhanced by GS 9-HE 4 phase.

602 The contraction of temperate forests is also recorded throughout MIS 3 in central Italy

603 (Lagaccione and Valle di Castiglione) and southern Italy at Lago Grande di Monticchio. In

604 these sites, open forests dominated by deciduous *Quercus*, *Corylus, Fagus, Tilia, Ulmus*

605 and *Carpinus betulus* experienced their maximum expansion between ca. 60-45 ka.

606 Afterwards, open environments (*Artemisia*-dominated steppe/ wooded steppe) expanded

607 between 45-30 ka (**Fig. 5**).

608 This general overview suggests latitudinal (and also altitudinal) climatic patterns and

609 rainfall gradients along the Italian peninsula due to its complex physiographic structure (i.e.

610 the presence of two high mountain ranges, Alps and Apennines), to be taken into account

611 when reconstructing past vegetation dynamics as it has already been shown for Greece

612 (Tzedakis et al., 2004).

613

614 **6 Archaeological framework**

615 During the first half of MIS 3, and particularly during GIs 14/13 ca. 55-48 ka, natural

616 environments were favourable for AMHs to migrate from Africa into Europe (Müller et al.,

617 2011). The scenario of an initial AMHs movement into Europe is supported by industries

618 associated with modern hominin remains found in few excavated localities: Üçağızlı cave

619 (Turkey) (Güleç et al., 2002; Kuhn et al., 2009); Ksar Akil (Lebanon) (Copeland and

620 Yazbeck, 2002; Yazbeck, 2004; Douka et al., 2013); Manot cave (Israel) (Hershkovitz et

621 al., 2015). Around 45 to 39 ka, Neandertals were replaced by AMHs (Higham et al., 2014),

622 and a variety of early Upper Palaeolithic cultures emerged (e.g., Uluzzian and Proto-

623 Aurignacian in the central-eastern Mediterranean regions; see Arrighi et al. and Marciani et

624 al., this issue).

625 The cultural complex known as Uluzzian has been attested in the Italian Peninsula and

626 southern Balkans around 45-40 ka (**Fig. 6**; Palma di Cesnola, 1989; Ronchitelli et al.,

627 2009; Moroni et al., 2013; Peresani, 2014; Zanchetta et al., 2018). This techno-complex

628 was coeval with the arrival of AMHs in Europe as evidenced by the anatomical features of

629 two deciduous teeth discovered in Grotta del Cavallo in Apulia (Benazzi et al., 2011,

630 although challenged by Zilhão et al., 2015, and further discussed in Moroni et al., 2018).

631 Along the Italian Peninsula, the Uluzzian is currently best known in cave sedimentary

632 successions by its stratigraphic position above the Mousterian and under the Proto-

633 Aurignacian, when the latter is present, and also in several open-air sites (**Fig. 6**).

634 Recently, the Uluzzian has also been observed in northern Italian cave sites, expanding its

635 cultural borders from what was thought to be exclusively central-southern after the

636 discovery of assemblages at Grotta Fumane and at the Riparo Broion shelter (Peresani,

637 2008; Peresani et al., 2016, 2018). Other sites in the Adriatic-Ionian region exhibit

638 Uluzzian elements (Crvena Stijena; Mihailović et al., 2017; Klissoura Cave; Starkovich,

639 2017; Kephalari; Darlas and Psathi, 2016), opening new perspectives in looking at the

640 appearance and spread of the Uluzzian over the entire area of the Adriatic basin.

641 In several sites from the Middle to Upper Palaeolithic transition is documented by the

642 Proto-Aurignacian technocomplex. The available chronological framework indicates a

643 Proto-Aurignacian occupation ending with the Campanian Ignimbrite eruption in Southern

644 Italian Castelcivita (Gambassini, 1997) and Serino sites (Lowe et al., 2012; Wood et al.,

645 2012). However, this tephrostratigraphic marker also constrains the end of the Uluzzian

646 techno-complexes at Grotta del Cavallo on the Ionic coast of Salento (Lecce) (Zanchetta

647 et al., 2018; section 7.2). In N-W Italy, the earliest Proto-Aurignacian is that of the Balzi

648 Rossi sites complex in the region of Liguria (NW Italy), where it has been identified at

649 Riparo Mochi and Riparo Bombrini sites (Douka et al., 2012; Riel-Salvatore and Negrino,

650 2018). At these sites, the main outlines of the industry remain stable beyond the end of

651 GS9/HE4 (Riel-Salvatore and Negrino, 2018), comparably to Grotta Fumane in the north

652 of Italy (Falcucci et al., 2017; Falcucci and Peresani, 2018). The assessment of these

653 temporal-spatial issues and new chronological information are fundamental for

654 understanding the dynamics of the cultural and ecological-anthropological changes that

655 occurred in S-Europe at the Middle to Upper Palaeolithic transition.

656 Already before 43 ka, very early Aurignacian assemblages, reflecting an initial AMHs

657 advance into central Europe, have also been found along the Danube (Willendorf II, Lower

658 Austria; Nigst et al., 2014), suggesting the Danube's role as a spatial corridor for human

659 dispersal in the Early Upper Palaeolithic (e.g., Floss, 2003; Hussain and Floss, 2016). A

660 similar role is hypothesized for the Don River system near the Black Sea (Anikovich et al.,

661 2007). Beside large river systems, also coastal plains played a relevant role channelling

662 AMHs dispersal into Europe (Mellars, 2006; Hublin, 2014). The close similarity between

663 the available dates for the early AMH arrival in the Mediterranean and in Germany on the

664 Danube, might suggest a rapid access in Europe via two routes, along both the Danube

665 corridor and the Mediterranean coasts (Douka et al., 2012).

666 # 7   Chronological issues

667 ## 7.1   Difficulties in dating the Middle to Upper Palaeolithic transition

668 Building reliable radiocarbon chronologies for sequences covering time intervals beyond

669 and/or close to the limit of the radiocarbon technique (i.e., ca. 50 ka) remain challenging.

670 Indeed, the low levels of residual ^{14}C activity induces lower precision (higher uncertainty)

671 and accuracy (higher offset of the measured isotope ratio with respect to the actual one) of

672 AMS measurements and makes samples much more vulnerable to contamination (e.g.,

673 Bird et al., 1999; Higham, 2011; Wood, 2015). In old samples, due to the low ^{14}C content,

674 even very negligible percentages of modern carbon give very high contamination levels

675 leading to wholly distorted chronologies, with resulting ages that can be younger of several

676 millennia (Higham et al., 2009; Higham, 2011). Indeed, this makes the dating of small

677 amounts of ancient carbon, i.e., more prone to contamination, even more challenging (e.g.,

678 Bird et al., 2014). Such problems can be partially overcome in long, continuous

679 sedimentary succession that are biostratigraphically well-constrained using indirect

680 approaches based on record alignment strategies, i.e., one record on a depth-scale is

681 aligned onto a "dated reference" record (Govin et al., 2015); provided that the underlying

682 assumptions, i.e., recognition of the events and their one-to-one correlation, are

683 reasonably demonstrated. Yet, whenever possible, tephra markers and/or relative

684 chronologies based on varved sediments can also be used to refine or validate age-

685 models.

686 ## 7.2   The Campanian Ignimbrite (CI) marker

687 The Campanian Ignimbrite (CI) super-eruption (southern Italy, ^{40}Ar/^{39}Ar age: 39.85 ± 0.14

688 ka, 2σ; ^{14}C age: 34.29 ± 0.09 ^{14}C ka BP, 1σ; Giaccio et al., 2017) produced the most

689 widespread tephra of western Eurasia, extending from the Tyrrhenian Sea to the Russian

690 Plain (e.g., Costa et al., 2012; Marti et al., 2016; **Fig. 7**). Its relevance as a key

691 chronological and stratigraphic marker for addressing a series of issues concerning the

692 European MIS 3 period – including the tempo and the palaeoecological factors involved in

693 the human bio-cultural evolution at the Middle-Upper Palaeolithic transition – has been

694 recognised long ago (e.g., Fedele et al., 2003) and eventually consolidated by a number of

695 papers: e.g., Giaccio et al., 2006 (see Higham et al., 2009 for the updated chronology of

696 Grotta Fumane); Pyle et al., 2006; Fedele et al., 2008; Giaccio et al., 2008; Hoffecker et

697 al., 2008; Lowe et al., 2012; Satow et al., 2015; Wutke et al., 2015; Wulf et al., 2018;

698 Zanchetta et al., 2018.

699 At several archaeological sites of the central Mediterranean, Balkans and Russian Plain

700 the CI tephra acts as a marker for the end of either final Mousterian with Uluzzian

701 elements (Crvena Stijena, Montenegro, Morley and Woodward, 2011; Mihajlovic and

702 Whallon, 2017), Uluzzian (Apulia region in southern-eastern Italy and Greece; e.g., Douka

703 et al., 2014; Zanchetta et al., 2018) or Proto-Aurignacian techocomplexes (e.g., Serino

704 open-air site and Castelcivita Cave in southern-western Italy and Kostenki site complex in

705 Russia; e.g., Giaccio et al., 2008 and references therein). However, although falling in its

706 dispersal area, the CI has not been detected at the Adriatic site of Grotta Paglicci (Apulia,

707 Southern Italy) and on the opposite Tyrrhenian side, at Grotta della Cala. In both caves the

708 Protoaurignacian seems to stretch beyond the CI event based on ^{14}C chronology (Paglicci)

709 and the studied materials (Marciani et al., this issue).

37

710   The CI tephra occurs in all the above-mentioned sites either as a relatively proximal, thick

711   primary pyroclastic succession (e.g., Serino open-air site; Accorsi et al., 1978; Giaccio et

712   al., 2006) or as a discrete layer, with a sharp lower contact with underling sediments,

713   made of purely volcanic material (i.e., glass shards or pumice fragments with mineral

714   accessories) with no or negligible contamination by clastic sediments. These features are

715   consistent with a sub-primary (re)deposition of ash layers by the wind or run-off shortly

716   after its emplacement as primary fallout along landforms nearby sheltered or open-air

717   archaeological sites (e.g., Brunis et al., 2019). Specifically, at Castelcivita site, both Plinian

718   pumice and co-ignimbritic ash layers are recorded in their eruptive stratigraphic order,

719   suggesting that the two eruptive units were transported and redeposited in the cave

720   immediately after their fall (fall and rolling process) (Giaccio et al., 2008; Giaccio et al.,

721   2016). The sub-primary nature of the CI tephra, i.e., no appreciable time elapsed between

722   CI tephra deposition and the eruption, is also supported by the available radiocarbon

723   chronology of the archaeological layers immediately below CI tephra strata, which are

724   statistically indistinguishable from the CI eruption age (Benazzi et al., 2011; Wood et al.,

725   2012; Douka et al., 2014; Giaccio et al., 2017). On the whole, both radiocarbon chronology

726   and CI tephra marker suggest that around 40 ka the central Mediterranean region was a

727   cultural, and possibly biological, mosaic, suggesting the possible coeval occurrence of the

728   final Mousterian (Crvena Stijena), Uluzzian (Apulia and Greece) and Protaurignacian lithic

729   technocomplexes (Campania).

730   Particularly significant is also the climatostratigraphic position of the CI tephra as revealed

731   by a number of marine and terrestrial palaeoclimatic records spread in the wide region of

732   its dispersal area (**Fig. 7**). In this framework, the palaeoecological and tephrostratigraphic

733   high-resolution (120 yr/sample) record of Tenaghi Philippon (Greece, Wulf et., al 2018)

734   offers the unique opportunity to compare the chronostratigraphic position of CI in relation

735   to the palaeoenvironmental context at a centennial scale during the Middle to Upper

736   Palaeolithic transition. In detail, CI deposition occurred ca. 1000 years after the onset of a

737   phase of marked arboreal pollen drop corresponding to the GS 9 (ca. 40.58 cal ka BP) and

738   3280 years before the onset of GI8 (ca. 36.3 cal ka BP) (**Fig. 7**; Wulf et al., 2018).

739   Similarly, at Monticchio site, the CI was deposited ca. 820 years after the onset of GS 9

740   (**Fig. 3**). However, at Tenaghi Philippon the resulting total duration of ca. 4280 years for

741   GS 9 strongly deviates from the ca. 2000 years obtained at Lago Grande di Monticchio

742   (Wutke et al., 2015) and from the 1680 years in the NGRIP record (i.e. from 39.90 to 38.22

743   ka GICC05; Rasmussen et al., 2014). A similar position is verified in number of other

744   terrestrial and marine palaeoenvironmental records (e.g., Mediterranean and Black Sea

745   marine records and Lake Ohrid, and Lesvos Island pollen profiles; see Giaccio et al., 2017

746   and references therein). Despite the general agreement in placing the CI well after the

747   beginning of GS 9 (ca. 400 years, according to the alignment of records proposed in

748   Giaccio et al., 2017), which is marked by a drop in arboreal pollen and temperate taxa

749   (**Fig. 7)**, it seems that further investigations are needed to fully disentangle temporal

750   discrepancies between records and to convincingly correlate the interval encompassing GI

751   8-10 to the D-O events. This is also challenging due to the inadequate resolution of most

752   of the available pollen records if compared to the short GI 9 duration (i.e., 250-yr-long

753   GICC05; Rasmussen et al., 2014), which only briefly interrupts the GS 10 to GS 9 interval

754   representing over 4 millennia of cold stadial conditions.

755 With specific regards to these chronological issues, it is worth noting that the paired, high-

756 precision, multiple $^{40}Ar/^{39}Ar$ and ^{14}C, ages for the CI revealed an offset of ca. 1 ka between

757 the calendar age of the CI as determined by its direct $^{40}Ar/^{39}Ar$ dating and the calibrated

758 ^{14}C age of the CI using IntCal13 calibration curve (Giaccio et al., 2017), thus highlighting

759 the occurrence of a further source of uncertainty when comparing records whose age

760 models are based on calibrated ^{14}C ages with others anchored to different time-scales

761 (e.g., U/Th or Greenland ice chronology). This offset is now confirmed by a recent study,

762 which reports a record of paired U/Th and ^{14}C ages from the Chinese Hulu Cave

763 stalagmite, continuously spanning the last 54 ka (Cheng et al., 2018). This new record also

764 reveals a radiocarbon plateau between ca. 37.5 ka and ca. 39.1 ka at ca. 33.5 ^{14}C ka BP

765 that could have affected the age model of records based on ^{14}C chronology and thus be

766 responsible for the above-mentioned notable age discrepancy in the length of the GS9 as

767 recorded in different Mediterranean records. A distortion of the IntCal13 calibration curve

768 at this time interval is also suggested by the recently published continuous record of the

769 $\Delta^{14}C$ spanning between ca. 47.3 and 39.6 ka cal. BP from the Tenaghi Philippon lake

770 succession (Staff et al., 2019).

771 All this information strictly related to this stratigraphic marker consolidate the notion of the

772 CI as a pivotal tool for deciphering and evaluating the potential interconnection between

773 climate, environmental, and human biological-cultural dynamics at the Middle to Upper

774 Palaeolithic transition, as well as in disentangling several temporal-spatial issues, crucial

775 for understanding the mechanisms underlying the interaction between AMHs and

776 Neandertals.

8   Concluding remarks and future developments

In this review, we summarized the current state of knowledge, also contributing with new elaborations of available data, on climate history, terrestrial ecosystems and palaeogeography, with the main aim to place Neanderthals and AMHs in the context of MIS 3 European landscape. Neanderthals lived in Eurasia alongside anatomically modern humans until ca. 40 ka. This overlap suggests direct or indirect contacts between the two species on a European sub-continental scale, potentially leading to interbreeding and cultural exchanges (Higham et al., 2014). To decipher the possible implications of climate variability and palaeoenvironmental transformation in such human processes, including Neanderthals extinction, two main aspects must be kept in mind: (i) the millennial/sub-millennial terrestrial response to high-frequency climate variability resulted in a pronounced and rapid alternation between forested and more open environments. Interestingly, the most relevant tree cover reductions in southern Europe are correlated to HEs, notably GS9-HE4; (ii) a long-term climatic trend (i.e., between ca. 50 and 25 ka) that led to dramatic increasing of the glaciers extent and lowering of the sea level, with major impacts on the coast landscape and on physiography and vegetation patterns. This implied the progressive development of effective ecological and physiographic barriers (i.e. the Alpine ice-dome) that limited connections between continental and Mediterranean Europe. In contrast, the gradual enlargement of coastlines and reorganization of European river systems may have played a key role in the migration processes.

To better understand and integrate these aspects, within the ERC - SUCCESS project, a Work Package is specifically dedicated. Studies will concentrate on the time span between Heinrich Event 5 to 3, known for their strong impact in Mediterranean Europe, the Balkans

41

800   and Italy (Follieri et al., 1988; Allen et al., 2000; Lézine et al., 2010; Pini et al., 2010; Müller

801   et al., 2011, Panagiotopoulos et al., 2014).

802   Attention will be paid to the reference record of Lake Fimon (Venetian Alpine foothills,

803   north-eastern Italy). This area is indeed well-known as it provides both a Late Pleistocene

804   palaeoecological record (Pini et al., 2010) and several Middle to Late Palaeolithic sites

805   yielding evidence of Neandertal and AMH occupation (Grotta Fumane and Riparo Broion

806   shelter; Peresani, 2011; **Fig. 3**). High-resolution palynostratigraphic researches are

807   currently in progress on the Lake Fimon core will be matched with archaeological

808   information from cave deposits in the same region to answer specific questions relevant to

809   the ERC Project, i.e. the effects of climate variability on the environments of last

810   Neandertals - early AMH, the role of fire, etc. Finally, to better comprehend regional

811   vegetation patterns and eco-climatic gradients across the Italian peninsula,

812   palaeoenvironmental proxies from Lake Fimon will be profitably compared to Central and

813   Southern Italian records, through the elaboration of available series and the investigation

814   of new sites.

815

Acknowledgements

821 helpful comments on Fig. 4 A. We also thank three anonymous reviewers and the editor

822 Dusan Boric for the valuable comments, which improved the quality of the manuscript.

823

References

825 Accorsi, C.A., Aiello, E., Bartolini, C., Castelletti I., Rodolfi, G., Ronchitelli A., 1978. Il
826 giacimento paleolitico di Serino (Avellino): stratigrafia, ambienti e paletnologia. Atti della
827 Società Toscana di Scienze Naturali, 86, 1979, 435-487.

828 Adamson, K.R., Woodward, J.C., Hughes, P.D., 2014. Glaciers and rivers: Pleistocene
829 uncoupling in a Mediterranean mountain karst. Quaternary Science Reviews 94, 28–43.

830 Alfano, M.J, Barron, E.J., Pollard, D., Huntley, B., Allen, J.R.M., 2003. Comparison of
831 climate model results with European vegetation and permafrost during oxygen isotope
832 stage three. Quaternary Research, 59, 97-107.

833 Allen, J.R.M., Brandt, U., Brauer A., Hubberten, H.-W., Huntley B., Keller, J., Kraml, M.,
834 Mackensen, A., Mingram, J., Negendank, J.F.W., Nowaczyk, N.R., Oberhänsli, H., Watts,
835 W.A., Wulf, S., Zolitschka, B., 1999. Rapid environmental changes in southern Europe
836 during the last glacial period. Nature, 400, 740-743.

837 Allen, J.R.M., Watts, W.A., Huntley, B., 2000. Weichselian palynostratigraphy,
838 palaeovegetation and palaeoenvironments; the record from Lago Grande di Monticchio,
839 southern Italy. Quaternary International, 73/74, 91-110.

840 Alvarez-Solas, J., Charbit S., Ritz, C., Paillard, D., Ramstein, G., Dumas, C., 2010. Links
841 between ocean temperature and iceberg discharge during Heinrich events. Nature
842 Geoscience, 3, 122-126.

843 Alvarez-Solas, J., Robinson, A., Montoya, M., Ritz, C., 2013. Iceberg discharges of the last
844 glacial period driven by oceanic circulation changes. PNAS, 110 (41): 16350-16354.

845 Andersen, K.K., Svensson, A., Johnsen, S.J., Rasmussen, S.O., Bigler, M., Röthlisberger,
846 R., Ruth, U., Siggaard-Andersen, M.L., Steffensen, J.P., Dahl-Jensen, D., Vinther, B.M.,
847 Clausen, H.B., 2006. The Greenland Ice Core chronology 2005, 15–42 kyr. Part 1:
848 Constructing the time scale, Quaternary Science Reviews, 25, 3246–3257.

849 Andrews, J. T., Voelker, A.H., 2018. "Heinrich events" (& sediments): A history of
850 terminology and recommendations for future usage. Quaternary Science Reviews, 187,
851 31-40.

852 Anikovich, M. V., Sinitsyn, A. A., Hoffecker, J. F., Holliday, V. T., Popov, V. V., Lisitsyn, S.
853 N., Forman, S. L., Levkovskaya, G. M., Pospelova, G. A., Kuz'mina, I. E., Burova, N. D.,
854 Goldberg, P., Macphail, R. I., Giaccio B., Praslov, N. D., 2007. Early Upper Paleolithic in
855 Eastern Europe and implications for the dispersal of modern humans. Science, 315
856 (5809), 223-226.

857 Antonioli, F., Vai, G.B., 2004 (Eds.). Litho-palaeoenvironmental Maps of Italy During the
858 Last Two Climatic Extremes. Climex Maps Italy e Explanatory Notes. Bologna, p. 80.

859 Antonioli, F., 2012. Sea level change in western-central Mediterranean since 300 kyr:
860 comparing global sea level curves with observed data. Alpine and Mediterranean
861 Quaternary, 25 (1), 15-23.

862 Archibold, O. W., 2012. Ecology of world vegetation. Springer Science & Business Media.

863 Arrighi, S., Moroni, A., Tassoni, L., Boschin, F., Badino, F., Bortolini, E., Boscato, P.,
864 Crezzini, J., Figus, C., Forte, M., Lugli F., Marciani, G., Oxilia G., Negrino F., Riel-
865 Salvatore J., Romandini, M., Spinapolice, E. E., Peresani, M., Ronchitelli, A., Benazzi, S.,
866 this issue. Bone tools, ornaments and other unusual objects during the Middle to Upper
867 Palaeolithic transition in Italy.

868 Bagniewski, W., Meissner, K.J., Menviel, L., 2017. Exploring the oxygen isotope fingerprint
869 of Dansgaard-Oeschger variability and Heinrich events. Quaternary Science Reviews,
870 159, 1-14.

871 Barker, S., Chen, J., Gong, X., Jonkers, L., Knorr, G., Thornalley, D., 2015. Icebergs not
872 the trigger for North Atlantic cold events. Nature, 520, 333-336.

873 Baroni, C., Guidobaldi, G., Salvatore, M.C., Christl, M., Ivy-Ochs, S., 2018. Last glacial
874 maximum glaciers in the Northern Apennines reflect primarily the influence of southerly
875 storm-tracks in the western Mediterranean. Quat. Sci. Rev. 197, 352-367.

876 Bartolomei, G., Broglio, A., Cattani, L., Cremaschi, M., Lanzinger, M., Leonardi, P.,1987-
877 88. Nuove ricerche nel deposito pleistocenico della Grotta di Paina sui Colli Berici
878 (Vicenza). Atti Istituto Veneto SS.LL.AA. CXLVI, 112-160.

879 Bar-Matthews, M., Ayalon, A., Kaufman, A., Wasserburg, G.J., 1999. The Eastern
880 Mediterranean paleoclimate as a reflection of regional events: Soreq cave, Israel. Earth
881 and Planetary Science Letters, 166 (1-2), 85-95.

882 Bar-Matthews, M., Avalon, A., Kaufman, A., 2000. Timing and hydrological conditions of
883 sapropel events in the Eastern Mediterranean as evident from speleothems, Soreq cave,
884 Israel. Chemical Geology, 169 (1-2), 145-156.

885 Bavec, M., Verbič, T., 2011. Glacial history of Slovenia. Dev. Quat. Sci. 15, 385–392.

886 Beaulieu, J.-L. de, Reille, M., 1984. A long upper Pleistocene pollen record from Les
887 Echets, near Lyon. Boreas, 1, 111-132.

888 Beaulieu, J.-L. de, Reille, M., 1992a. The last climatic cycle at La Grand Pile (Vosges,
889 France). A new pollen profile. Quaternary Science Reviews, 11, 431–438.

45

890 Beaulieu, J.-L. de, Reille, M., 1992b. Long Pleistocene sequences from the Velay plateau

891 (Massif Central, France). I. Ribains maar. Vegetation History and Archaeobotany, 1, 233–

892 242.

893 Becker, D., Verheul, J., Zickel, M., Willmes, C., 2015. LGM paleoenvironment of Europe –

894 Map. CRC806-Database, DOI: http://dx.doi.org/10.5880/SFB806.15.

895 Been, E., Hovers, E., Ekshtain, R., Malinsky-Buller, A., Agha, N., Barash, A., Bar-Yosef

896 Mayer, D.E., Benazzi S., Hublin, J-J., Levin, L., Greenbaum N., Mitki, N., Oxilia G., Porat,

897 N., Roskin, J., Soudack, M., Yeshurun, R., Shahack-Gross, R., Nir, N., Stahlschmidt, M.C.,

898 Rak, Y., Barzilai, O., 2017. The first Neanderthal remains from an open-air Middle

899 Palaeolithic site in the Levant. Scientific Reports, 7, 2958.

900 Benazzi, S, Douka, K, Fornai, C, Bauer, C. C., Kullmer, O, Svoboda, J, Pap, I., Mallegni,

901 F., Bayle, P., Coquerelle, M., Condemi, S., Ronchitelli, A., Harvati, K., Weber, G. W., 2011.

902 Early dispersal of modern humans in Europe and implications for Neanderthal behaviour.

903 Nature 479, 525–528.

904 Benazzi, S., Slon, S., Talamo, S., Negrino, F., Peresani, M., Bailey, S.E., Sawyer, S.,

905 Panetta, D., Vicino, G., Starnini, E., Mannino, M.A., Salvadori, P.A., Meyer, M., Pääbo, S.,

906 Hublin, J-J., 2015. The Makers of the Protoaurignacian and Implications for Neandertal

907 Extinction. Science 348, 793-6.

908 Benini, A., Boscato, P., Gambassini, P., 1997. Grotta della Cala (Salerno): industrie litiche

909 e faune uluzziane e aurignaziane. Rivista di Scienze Preistoriche 48, 37–95.

910 Bird, M.I., Ayliffe, L.K., Fifield, L.K., Turney, C.S.M., Cresswell, R.G., Barrows, T.T., David,

911 B., 1999. Radiocarbon dating of "old" charcoal using a wet oxidation, stepped-combustion

912 procedure. Radiocarbon, 41 (2), 127-140.

913 Bird, M.I., Levchenko, V., Ascough, P.L., Meredith, W., Wurster, C.M., Williams, A.,

914 Tilston, E.L., Snape, C.E., Apperley, D.C., 2014. The efficiency of charcoal

915   decontamination for radiocarbon dating by three pre-treatments–ABOX, ABA and
916   hypy. Quaternary Geochronology, 22, 25-32.

917   Blockley, S.P.E., Lane, C.S., Hardiman, M., Rasmussen, S.O., Seierstad, I.K., Steffensen,
918   J.P., Svensson, A., Lotter, A.F., Turney, C.S.M., Bronk Ramsey, C., 2012. Synchronisation
919   of palaeoenvironmental records over the last 60,000 years, and an extended INTIMATE
920   event stratigraphy to 48,000 b2k. Quaternary Science Reviews 36, 2-10.

921   Bond, G., Heinrich, H., Broecker, W., Labeyrie, L., McManus, J., Andrews, J., Huon, S.,
922   Jantschik, R., Clasen, S., Simet, C., Tedesco, K., Klas, M., Bonani, G., and Ivy, S., 1992.
923   Evidence for massive discharges of icebergs into the North Atlantic ocean during the last
924   glacial period, Nature, 360, 245–249.

925   Bond, G., Broecher, W., Johnsen, S.J., MacManus, J., Laberie, L., Jouzel, J., Bonani, G.,
926   1993. Correlations between climate records from North Atlantic sediments and Greenland
927   ice, Nature, 365, 143–147.

928   Boretto, G., Zanchetta, G., Ciulli, L., Bini, M., Fallick, E., Lezzerini, M., Colonese A.C.,
929   Zembo, I., Trombino, L., Regattieri, E., Sarti, G., 2017. The loess deposits of Buca Dei
930   Corvi section (Central Italy): Revisited. Catena, 151, 225-237.

931   Borzatti von Löwenstern, E., 1965. La grotta di Uluzzo (campagna di scavi 1964). Rivista
932   di Scienze Preistoriche 19, 41-52.

933   Borzatti von Löwenstern, E., 1966. Alcuni aspetti del Musteriano nel Salento. (La grotta-
934   riparo di Torre dell'Alto e la grotta di Uluzzo C). Scavi 1965 e 1966. Rivista di Scienze
935   Preistoriche 21, 203–287.

936   Borzatti von Löwenstern, E., 1970. Prima campagna di scavi nella grotta "Mario
937   Bernardini" (Nardò - Lecce). Rivista di Scienze Preistoriche 25, 89–125.

938 Broecker, W.S.T., Peng, H., Jouzel, J., Russell, G., 1990. The magnitude of global fresh-
939 water transports of importance to ocean circulation. Climate Dynamics, 4, 73-79.

940 Bruins, H. J., Keller, J., Klügel, A., Kisch, H. J., Katra, I., van der Plicht, J., 2019. Tephra in
941 caves: Distal deposits of the Minoan Santorini eruption and the Campanian super-eruption.
942 Quaternary International, 499, 135-147.

943 Buoncristiani, J.-F., Campy, M. 2004. Palaeogeography of the last two glacial episodes in
944 the Massif Central, France. Dev. Quat. Sci. 2, 111-112.

945 Burjachs, F., López-García, J.M., Allué, E., Blain, H.A., Rivals, F., Bennàsar, M., Expósito,
946 I., 2012. Palaeoecology of Neanderthals during Dansgaard–Oeschger cycles in
947 northeastern Iberia (Abric Romaní): from regional to global scale. Quaternary
948 International, 247, 26-37.

949 Butzin, M., Köhler, P., Lohmann, G., 2017. Marine radiocarbon reservoir age simulations
950 for the past 50,000 years. Geophysical Research Letters, 44 (16), 8473-8480.

951 Cacho, I., Grimalt, J. O., Pelejero, C., Canals, M., Sierro, F. J., Flores, J. A., Shackleton,
952 N., 1999. Dansgaard-Oeschger and Heinrich event imprints in Alboran Sea
953 paleotemperatures. Paleoceanography, 14 (6), 698-705.

954 Carraro F., Sauro U., 1979. Il Glacialismo "locale" Wurmiano del Massiccio del Grappa
955 (Provincie di Treviso e di Vicenza). Geografia Fisica e Dinamica Quaternaria, 2(1), 6-16.

956 Cattani L., Renault-Miskovsky, J., 1983-84. Etude pollinique du remplissage de la Grotte
957 du Broion (Vicenza, Italie). Paléoclimatologie du Würmien en Vénétie. Bullettin Association
958 Française Étude du Quaternaire, XVI (4), 197-212.

959 Cattani, L., 1990. Steppe environments at the margin of the Venetian Pre-Alps during the
960 Pleniglacial and Late-Glacial periods. In: Cremaschi M. (ed), The Loess in Northern and

961   Central Italy: a Loess Basin between the Alps and the Mediterranean Region, Quaderni di

962   Geodinamica Alpina e Quaternaria., 1: 133-137.

963   Cheng, H., Lawrence Edwards, R., Southon, J., Matsumoto, K., Feinberg, J.M., Sinha, A.,

964   Zhou, W., Li, H., Li, X., Xu, Y., Chen, S., Tan, M., Wang, Q., Wang, Y., Ning, Y., 2018.

965   Atmospheric ^{14}C/^{12}C changes during the last glacial period from Hulu Cave. Science, 362,

966   1293-1297.

967   Chiesa, S., Coltorti, M., Cremaschi, M., Ferraris, M., Prosperi, I., 1990. Loess sedimenta-

968   tion and quaternary deposits in the Marche province. In Cremaschi, M. (Ed.), The loess in

969   northern and central Italy. A loess basin between the Alps and the Mediterranean region,

970   Quaderni di Geodinamica Alpina e Quaternaria 1, Milano, 103-130.

971   Combourieu-Nebout, N., Turon, J.-L., Zahn, R., Capotondi, L., Londeix, L., Pahnke, K.,

972   2002. Enhanced aridity and atmospheric high-pressure stability over the western

973   Mediterranean during the North Atlantic cold events of the past 50 k.y. Geology 30, 863–

974   866.

975   Combourieu-Nebout, N., Peyron, O., Dormoy, I., Desprat, S., Beaudouin, C., Kotthoff, U.,

976   Marret, F., 2009. Rapid climatic variability in the west Mediterranean during the last 25 000

977   years from high resolution pollen data. Climate of the Past, 5 (3), 503-521.

978   Copeland, L., Yazbeck, C., 2002. Inventory of Stone Age Sites in Lebanon. In: New and

979   Revised, Part III, vol. 55. Melanges de l'Universite Saint-Joseph, 121-325.

980   Costa, A., Folch, A., Macedonio, G., Giaccio, B., Isaia, R., Smith, V.C., 2012. Quantifying

981   volcanic ash dispersal and impact of the Campanian Ignimbrite super-eruption.

982   Geophysical Research Letters, 39 (10).

983   Cremaschi, M., 1990. The loess in northern and central Italy. A loess basin between the

984   Alps and the Mediterranean region. Quaderni di Geodinamica Alpina e Quaternaria 1,

985   Milano, Italy.

986   Cremaschi, M., 2004. Late Pleistocene loess. In: Antonioli, F., Vai, G.B. (Eds.), Litho-
987   palaeoenvironmental Maps of Italy During the Last Two Climatic Extremes. Climex Maps
988   Italy e Explanatory Notes. Bologna, 34–37.

989   Cremaschi, M., Zerboni, A., Nicosia, C., Negrino, F., Rodnight, H., Spötl, C., 2015. Age,
990   soil-forming processes, and archaeology of the loess deposits at the Apennine margin of
991   the Po Plain (northern Italy). New insights from the Ghiardo area. Quaternary International,
992   376, 173–188.

993   Cremonesi, G., 1987. Due complessi d'arte del Paleolitico superiore: la Grotta Polesini e la
994   Grotta delle Veneri. Atti del VI Convegno di Preistoria e Protostoria. Storia della Daunia, 2,
995   35-50.

996   Crouvi, O., Amit, R., Enzel, Y., Gillespie, A.R., 2010. The role of active sand seas in the
997   formation of desert loess. Quaternary Science Reviews, 29, 2087–2098.

998   Daniau, A. L., Sánchez-Goñi, M. F., Beaufort, L., Laggoun-Défarge, F., Loutre, M. F.,
999   Duprat, J., 2007. Dansgaard–Oeschger climatic variability revealed by fire emissions in
1000   southwestern Iberia. Quaternary Science Reviews, 26(9-10), 1369-1383.

1001   Daniau, A. L., Goñi, M.F.S., Duprat, J., 2009. Last glacial fire regime variability in western
1002   France inferred from microcharcoal preserved in core MD04-2845, Bay of Biscay.
1003   Quaternary Research, 71(3), 385-396.

1004   Dansgaard, W., Johnsen, S.J., Clausen, H.B., Dahl-Jensen, D., Gundestrup, N.S.,
1005   Hammer, C.U., Hvidberg, C.S., Steffensen, J.P., Sveinbjorndottir, A.E., Jouzel, J., Bond,
1006   G., 1993. Evidence for general instability of past climate from a 250-kyr ice-core record.
1007   Nature, 364, 218-220.

1008   Darfeuil, S., Ménot, G., Giraud, X., Rostek, F., Tachikawa, K., Garcia, M., Bard, É., 2016.
1009   Sea surface temperature reconstructions over the last 70 kyr off Portugal: Biomarker data
1010   and regional modeling. Paleoceanography, 31 (1), 40-65.

1011 Darlas, A., Psathi, E., 2016. The Middle and Upper Paleolithic on the western coast of the
1012 Mani Peninsula (southern Greece). In Paleoanthropology of the Balkans and Anatolia (pp.
1013 95-117). Springer, Dordrecht.

1014 de Goěr, H. 1972. La Planèze de Saint Flour: formes et dépots glaciaires. Annales de la
1015 faculté des Sciences de Clermont-Ferrand, 48, 1-204.

1016 Delmas, M., 2015. The Last Maximum Ice Extent and subsequent deglaciation of the
1017 Pyrenees: an overview of recent research. Cuadernos de Investigación Geográfica, 41,
1018 359-387.

1019 Delpiano, D., Peresani, M., Bertola, S., Cremaschi, M., Zerboni, A., 2019. Lashed by the
1020 wind: short-term Middle Palaeolithic occupations within the loess-palaeosoil sequence at
1021 Monte Netto (Northern Italy). Quaternary International, 502, 137-147.

1022 Dini, M., Tozzi, C., 2012. La Transizione Paleolitico Medio-Paleolitico Superiore nella
1023 Grotta La Fabbrica (Grosseto-Toscana). Atti della Società Toscana di Scienze Naturali -
1024 Memorie Serie A, 117-119.

1025 Douka, K., Higham, T. F., Wood, R., Boscato, P., Gambassini, P., Karkanas, P., Peresani,
1026 M., Ronchitelli, A. M., 2014. On the chronology of the Uluzzian. Journal of Human
1027 Evolution, 68, 1-13.

1028 Douka, K., Grimaldi, S., Boschian, G., del Lucchese, A., Higham, T. F., 2012. A new
1029 chronostratigraphic framework for the Upper Palaeolithic of Riparo Mochi (Italy). Journal of
1030 Human Evolution, 62 (2), 286-299.

1031 Douka, K., Bergman, C.A., Hedges, R.E.M., Wesselingh, F.P., Higham, T., 2013.
1032 Chronology of Ksar Akil (Lebanon) and implications for the colonization of Europe by
1033 anatomically modern humans. PLoS ONE, 8, e72931.

1034 Douka, K., Higham, T., 2017. The chronological factor in understanding the Middle and

1035 Upper Paleolithic of Eurasia. Current Anthropology, 58 (S17), S480-S490.

1036 Drescher-Schneider, R., Jacquat, C., Schoch, W., 2007. Palaeobotanical investigations at

1037 the mammoth site of Niederweningen (Kanton Zürich). Switzerland. Quaternary

1038 International, 164-165, 113-129.

1039 Ehlers, J., Gibbard, P.L., Hughes, P.D., 2011. Quaternary Glaciations e Extent and

1040 Chronology, vol. 15. Elsevier, Amsterdam, 1126.

1041 Engel, Z., Mentlík, P., Braucher, R., Minár, J., Léanni, L., Aster Team, 2015.

1042 Geomorphological evidence and ^{10}Be exposure ages for the last glacial maximum and

1043 deglaciation of the Velká and Malá Studená dolina valleys in the high Tatra mountains,

1044 central Europe. Quaternary Science Reviews 124, 106-123.

1045 European Environment Agency, 2015. European ecosystem assessment - concept, data,

1046 and implementation. Contribution to Target 2 Action 5 Mapping and Assessment of

1047 Ecosystems and their Services (MAES) of the EU Biodiversity Strategy to 2020. Technical

1048 Report 06/2015.

1049 Falcucci, A., Conard, N.J., Peresani, M., 2017. A critical assessment of the

1050 Protoaurignacian lithic technology at Fumane Cave and its implications for the definition of

1051 the earliest Aurignacian. PloS ONE, 12 (12), e0189241.

1052 Falcucci, A., Peresani, M., 2018. Protoaurignacian core reduction procedures: blade and

1053 bladelet technologies at Fumane Cave. Lithic Technology, 43(2), 125-140.

1054 Farquhar, G.D., 1997. Carbon dioxide and vegetation, Science, 278 (5342), 1411.

1055 Fedele, F.G., Giaccio, B., Isaia, R., Orsi, G., 2003. The Campanian Ignimbrite eruption,

1056 Heinrich Event 4, and the Paleolithic change in Europe: a high-resolution investigation.

1057   Volcanism and Earth's Atmosphere, eds Robock A., Oppenheimer C. (AGU Geophys,

1058   Washington, DC), 301–325.

1059   Fedele, F.G., Giaccio, B., Hajdas, I., 2008. Timescales and cultural process at 40,000 BP

1060   in the light of the Campanian Ignimbrite eruption, western Eurasia. Journal of Human

1061   Evolution, 55, 834–857.

1062   Ferraro, F., 2009. Age, sedimentation, and soil formation in the Val Sorda loess sequence,

1063   Northern Italy. Quaternary International, 204, 54–64.

1064   Fischer, H., Fundel, F., Ruth, U., Twarloh, B., Wegner, A., Udisti, R., Becagli, S.,

1065   Castellano, E., Morganti, A., Severi, M., Wolff, E., Littot G., Röthlisberger, R., Mulvaney,

1066   R., Hutterli, M. A., Kaufmann, P., Federer, U., Lambert, F., Bigler M., Hansson, M., Jonsell,

1067   U., de Angelis, M., Boutron, C., Siggaard-Andersen, M.-L., Steffensen, J. P., Barbante, C.,

1068   Gaspari, V., Gabrielli, P., Wagenbach, D., 2007a. Reconstruction of millennial changes in

1069   dust emission, transport and regional sea ice coverage using the deep EPICA ice cores

1070   from the Atlantic and Indian Ocean sector of Antarctica. Earth and Planetary Science

1071   Letters, 260 (1), 340-354.

1072   Fischer, H., Siggaard-Andersen, M.L., Ruth, U., Röthlisberger, R., Wolff, E., 2007b.

1073   Glacial/interglacial changes in mineral dust and sea-salt records in polar ice cores:

1074   Sources, transport, and deposition. Reviews of Geophysics, 45 (1).

1075   Fleitmann, D., Cheng, H., Badertscher, S., Edwards, R.L., Mudelsee, M., Göktürk, O.M.,

1076   Fankhauser A., Pickering R., Raible C.C., Matter A, Kramers J, Tüysüz O., 2009. Timing

1077   and climatic impact of Greenland interstadials recorded in stalagmites from northern

1078   Turkey. Geophysical Research Letters, 36 (19).

1079   Fletcher, W.J., Sánchez Goñi, M.F., 2008. Orbital-and sub-orbital-scale climate impacts on

1080   vegetation of the western Mediterranean basin over the last 48,000 yr. Quaternary

1081   Research, 70 (3), 451-464.

53

1082 Fletcher, W.J., Sánchez Goñi, M.F., Peyron, O., Dormoy, I., 2010a. Abrupt climate
1083 changes of the last deglaciation detected in a Western Mediterranean forest record.
1084 Climate of the Past, 6, 245-264.

1085 Fletcher, W.J., Sánchez Goñi, M. F., Allen, J. R. M., Cheddadi, R., Comborieu-Nebout, N.,
1086 Huntley, B., Lawson, I., Londeix, L., Magri, D., Margari, V., Müller, U. C., Naughton, F.,
1087 Novenko, E., Roucoux, K., Tzedakis, P.C., 2010b. Millennial scale variability during the
1088 last glacial in vegetation records from Europe. Quaternary Science Reviews. Quaternary
1089 Science Reviews, 29 (21-22), 2839-2864.

1090 Floss, H., 2003. Did they meet or not? Observations on Châtelperronian and Aurignacian
1091 settlement patterns in eastern France. In (Zilhao & Errico, eds): The chronology of the
1092 Aurignacian and of the transitional technocomplexes. Dating, stratigraphies, cultural
1093 implications. Actes 14e Congrès UISPP, Université de Liège, Belgique, 2-8 sept. 2001.
1094 Trabalhos de Arqueologia n° 33, 273-287.

1095 Flückiger, J., Knutti, R., White, J.W., 2006. Oceanic processes as potential trigger and
1096 amplifying mechanisms for Heinrich events. Paleoceanography, 21 (2).

1097 Follieri, M., Magri, D., Sadori, L., 1988. 250,000-year pollen record from Valle di
1098 Castiglione (Roma). Pollen et Spores 30, 329-356.

1099 Follieri, M., Giardini, M., Magri, D., Sadori, L., 1998. Palynostratigraphy of the last glacial
1100 period in the volcanic region of central Italy. Quaternary International, 47, 3-20.

1101 Fontana, A., Mozzi, P., Marchetti, M., 2014. Alluvial fans and megafans along the southern
1102 side of the Alps. Sediment. Geol. 301, 150–171.

1103 Forno, M.G., Gianotti, F., Racca, G. 2010. Significato paleoclimatico dei rapporti tra il
1104 glacialismo principale e quello tributario nella bassa Valle della Dora Baltea. Il Quaternario
1105 23, 105-124.

1106 Franciscus, R.G., 1999. Neandertal nasal structures and upper respiratory tract
1107 "specialization". Proceedings of the National Academy of Sciences, 96 (4), 1805-1809.

1108 Frechen, M., Horváth, E., Gábris, G., 1997. Geochronology of Middle and Upper
1109 Pleistocene loess sections in Hungary. Quaternary Research, 48, 291–312.

1110 Furlanetto, G., Ravazzi, C., Badino, F., Brunetti, M., Champvillair, E., Maggi, V., 2019.
1111 Elevational transects of modern pollen samples: Site-specific temperatures as a tool for
1112 palaeoclimate reconstructions in the Alps. The Holocene, 29(2), 271-286.

1113 Gambassini, P., 1997. Il Paleolitico di Castelcivita: culture e ambiente. Electa, Napoli, Italy.

1114 Genty, D., Blamart, D., Ouahdi, R., Gilmour, M., Baker, A., Jouzel, J., Van-Exter, S., 2003.
1115 Precise dating of Dansgaard–Oeschger climate oscillations in western Europe from
1116 stalagmite data. Nature, 421 (6925), 833.

1117 Genty, D., Blamart, D., Ghaleb, B., Plagnes, V., Causse, C., Bakalowicz, M., Zouari, K.,
1118 Chkir N., Hellstrom, J., Wainer, K., Bourges, F., 2006. Timing and dynamics of the last
1119 deglaciation from European and North African δ^{13}C stalagmite profiles—comparison with
1120 Chinese and South Hemisphere stalagmites. Quaternary Science Reviews, 25 (17-18),
1121 2118-2142.

1122 Genty, D., Combourieu-Nebout, N., Peyron, O., Blamart, D., Wainer, K., Mansuri, F.,
1123 Ghaleb, B., Isabello, L., Dormoy, I., von Grafenstein, U., Bonelli, S., Landais A., Brauer, A.,
1124 2010. Isotopic characterization of rapid climatic events during OIS3 and OIS4 in Villars
1125 Cave stalagmites (SW-France) and correlation with Atlantic and Mediterranean pollen
1126 records. Quaternary Science Reviews, 29 (19), 2799-2820.

1127 Giaccio, B., Hajdas, I., Peresani, M., Fedele, F.G., Isaia, R., 2006. The Campanian
1128 Ignimbrite tephra and its relevance for the timing of the Middle to Upper Palaeolithic shift.
1129 When Neanderthals and Modern Humans Met, ed Conard N.J. (Kerns Verlag, Tübingen,
1130 Germany), 343–375.

55

1131 Giaccio, B., Isaia, R., Fedele, F.G., Di Canzio, E., Hoffecker, J., Ronchitelli, A., Sinitsyn,
1132 A.A., Anikovich, M., Lisitsyn S.N., Popov, V.V. 2008. The Campanian Ignimbrite and
1133 Codola tephra layers: Two temporal/stratigraphic markers for the Early Upper Palaeolithic
1134 in southern Italy and eastern Europe. Journal of Volcanology and Geothermal Research,
1135 177, 208–226.

1136 Gianotti, F., Forno, M.G., Ivy-Ochs S., Monegato, G., Pini, R., Ravazzi, C., 2015.
1137 Stratigraphy of the Ivrea morainic amphitheatre (NW Italy): an updated synthesis. Alpine
1138 and Mediterranean Quaternary, 28, 29-58.

1139 Giaccio, B., Hajdas, I., Isaia, R., Deino, A., Nomade, S., 2017. High-precision ^{14}C and
1140 ^{40}Ar/^{39}Ar dating of the Campanian Ignimbrite (Y-5) reconciles the time-scales of climatic-
1141 cultural processes at 40 ka. Scientific reports, 7, 45940.

1142 Giraudi, C., Giaccio, B., 2016. Middle Pleistocene glaciations in the Apennines, Italy: new
1143 chronological data and preservation of the glacial record. In: Hughes, P.D. & Woodward,
1144 J.C. (eds) Quaternary Glaciation in the Mediterranean Mountains. Geological Society,
1145 London, Special Publications, 433, 161-178.

1146 Govin, A., Capron, E., Tzedakis, P.C., Verheyden, S., Ghaleb, B., Hillaire-Marcel, C., St-
1147 Onge, G., Stoner, J.S., Bassinot, F., Bazin, L., Blunier, T., Combourieu-Nebout, N., El
1148 Ouahabi, A., Genty, D., Gersonde, R., Jimenez-Amat, P., Landais, A., Martrat, B.,
1149 Masson-Delmotte, V., Parrenin, F., Seidenkrantz, M.-S., Veres, D., Waelbroeck, C., Zahn,
1150 R., 2015. Sequence of events from the onset to the demise of the Last Interglacial:
1151 Evaluating strengths and limitations of chronologies used in climatic archives. Quaternary
1152 Science Reviews, 129, 1-36.

1153 Grant, K.M., Rohling, E.J., Bar-Matthews, M., Ayalon, A., Medina-Elizalde, M., Ramsey, C.
1154 B., Satow, C., Roberts, A.P., 2012. Rapid coupling between ice volume and polar
1155 temperature over the past 150,000 years. Nature, 491 (7426), 744.

1156 Greenbaum, G., Friesem, D. E., Hovers, E., Feldman, M. W., Kolodny, O., 2018. Was

1157 inter-population connectivity of Neanderthals and modern humans the driver of the Upper

1158 Paleolithic transition rather than its product?. Quaternary Science Reviews.

1159 Gromig, R., Mechernich, S., Ribolini, A., Wagner, B., Zanchetta, G., Isola, I., Bini, M.,

1160 Dunai, T., 2018. Evidence for a Younger Dryas deglaciation in the Galicica Mountains

1161 (FYROM) from cosmogenic ^{36}Cl. Quaternary International, 464, 352–363.

1162 Guillevic, M., Bazin, L., Landais, A., Stowasser, C., Masson-Delmotte, V., Blunier, T.,

1163 Eynaud, F., Falourd, S., Michel, E., Minster, B., Popp, T., Prié, F., Vinther, B. M., 2014.

1164 Evidence for a three-phase sequence during Heinrich Stadial 4 using a multiproxy

1165 approach based on Greenland ice core records. Climate of the Past, 10 (6), 2115-2133.

1166 Guiot, J., Reille, M., Beaulieu, J.L. de, Pons, A., 1992. Calibration of the climatic signal in a

1167 new pollen sequence from La Grande Pile. Climate Dynamics, 6 (3-4), 259-264.

1168 Güleç, E., Kuhn, S.L., Stiner, M. C., 2002. The early Upper Palaeolithic of Üçağızlı Cave,

1169 Turkey. Antiquity, 76 (293), 615-616.

1170 Haase, D., Fink, J., Haase, G., Ruske, R., Pécsi, M., Richter, H., Altermann, M., Jäger, K.

1171 D., 2007. Loess in Europe - its spatial distribution based on a European Loess Map, scale

1172 1: 2,500,000. Quaternary Science Reviews, 26 (9-10), 1301-1312.

1173 Haesaerts, P., Borziac, I., Chekha, V.P., Chirica, V., Damblon, F., Drozdov, N.I., Orlova,

1174 L.A., Pirson, S., van der Plicht, J., 2009. Climatic signature and radiocarbon chronology of

1175 middle and late pleniglacial loess from Eurasia: comparison with the marine and

1176 Greenland records. Radiocarbon, 51 (1), 301-318.

1177 Harrison, S.P., Sánchez Goñi, M.F., 2010. Global patterns of vegetation response to

1178 millennial-scale variability and rapid climate change during the last glacial

1179 period. Quaternary Science Reviews, 29 (21-22), 2957-2980.

57

1180 Heinrich, H., 1988. Origin and consequences of cyclic ice rafting in the northeast Atlantic

1181 Ocean during the past 130,000 years. Quaternary research, 29 (2), 142-152.

1182 Heiri, O., Koinig, K.A., Spötl, C., Barrett, S., Brauer, A., Drescher-Schneider, R.,G. Dorian,

1183 Ivy-Ochs, S., Kerschner, H., Luetscher, M., Moran, A., Nicolussi, K., Preusser, F.,

1184 Schmidt, R., Schoeneich, P., Schwörer, C., Sprafke, T., Terhorst, B., Tinner, W., 2014.

1185 Palaeoclimate records 60–8 ka in the Austrian and Swiss Alps and their

1186 forelands. Quaternary Science Reviews, 106, 186-205.

1187 Hemming, S.R., 2004. Heinrich events: Massive late Pleistocene detritus layers of the

1188 North Atlantic and their global climate imprint. Reviews of Geophysics, 42 (1), RG1005,

1189 doi:10.1029/2003RG000128.

1190 Hershkovitz, I., Marder, O., Ayalon, A., Bar-Matthews, M., Yasur, G., Boaretto, E.,

1191 Caracuta V., Alex, B., Frumkin, A., Goder-Goldberger, M., Gunz, P., Holloway, R.L.,

1192 Latimer, B., Lavi, R., Matthews, A., Slon, Vi., Bar-Yosef Mayer, D., Berna, F., Bar-Oz, G.,

1193 Yeshurun, R., May, H., Hans, M.G., Weber, G.W., Barzilai, O., 2015. Levantine cranium

1194 from Manot Cave (Israel) foreshadows the first European modern humans. Nature, 520

1195 (7546), 216.

1196 Higham, T., Brock, F., Peresani, M., Broglio, A., Wood, R., Douka, K., 2009. Problems with

1197 radiocarbon dating the Middle to Upper Palaeolithic transition in Italy. Quaternary Science

1198 Reviews, 28 (13-14), 1257-1267.

1199 Higham, T., 2011. European Middle and Upper Palaeolithic radiocarbon dates are often

1200 older than they look: problems with previous dates and some remedies. Antiquity, 85

1201 (327), 235-249.

1202 Higham, T., Douka, K., Wood, R., Ramsey, C.B., Brock, F., Basell, L., Camps, M.,

1203 Arrizabalaga, A., Baena, J., Barroso-Ruiz, C., Bergman, C., Boitard, C., Boscato, P.,

1204 Caparros, M., Conard, N. J., Draily, C., Froment, A., Galvan, B., Gambassini, P., Garcia-

1205 Moreno, A., Grimaldi, S., Haesaerts, P., Holt, B., Iriarte-Chiapusso, M. J., Jelinek, A.,

1206   Jorda Pardo, J.F., Maillo-Fernandez, J.M., Marom, A., Maroto J, Menendez M, Metz L,

1207   Morin E, Moroni, A., Negrino, F., Panagopoulou, E., Peresani, M., Pirson, S., de la Rasilla,

1208   M., Riel-Salvatore, J., Ronchitelli, A., Santamaria, D., Semal, P., Slimak, L., Soler, J.,

1209   Soler, N., Villaluenga, A., Pinhasi, R., Jacobi, R., 2014. The timing and spatiotemporal

1210   patterning of Neanderthal disappearance. Nature 512, 306-309.

1211   Hoffecker, J.F., Holliday, V.T., Anikovich, M. V., Sinitsyn, A.A., Popov, V.V., Lisitsyn, S.N.,

1212   Levkovskaya, G.M., Pospelova, G.A., Forman, S.L., Giaccio, B., 2008. From the bay of

1213   Naples to the River Don: The Campanian Ignimbrite eruption and the Middle to Upper

1214   Paleolithic transition in eastern Europe. Journal of Human Evolution, 55, 858–70.

1215   Hoffecker, J.F., 2009. The spread of modern humans in Europe. Proceedings of the

1216   National Academy of Sciences, 106 (38), 16040-16045.

1217   Holtmeier, F. K.,1985. Climatic stress influencing the physiognomy of trees at the polar

1218   and mountain timberline. Eidgenössische Anstalt für das Forstliche Versuchswesen,

1219   Berichte 270, 31–40.

1220   Holtmeier, F. K., 2009. Mountain timberlines: ecology, patchiness, and dynamics (Vol. 36).

1221   Springer Science & Business Media.

1222   Hublin, J.-J., 2014. The modern human colonization of western Eurasia: when and where?

1223   Quaternary Science Reviews, 1–17.

1224   Hublin, J-J., 2015. The Modern Human Colonization of Western Eurasia: When and

1225   Where? Quaternary Science Reviews, 18, 194–210.

1226   Hughes, A.L.C., Gyllencreutz, R., Lohne, Ø.S., Mangerud, J., Svendsen, J.I., 2016. The

1227   last Eurasian ice sheets - a chronological database and time-slice reconstruction, DATED-

1228   1. Boreas, 45, 1-45.

1229 Hughes, P.D., Woodward, J.C., 2016. Quaternary glaciation in the Mediterranean
1230 mountains: a new synthesis. In: Hughes, P.D. & Woodward, J.C. (eds) Quaternary
1231 Glaciation in the Mediterranean Mountains. Geological Society, London, Special
1232 Publications, 433, pp. 1-23. doi.org/10.1144/SP433.14

1233 Hussain, S. T., Floss, H., 2016. Streams as entanglement of nature and culture: European
1234 Upper Paleolithic river systems and their role as features of spatial organization. Journal of
1235 archaeological method and theory, 23(4), 1162-1218.

1236 Iglesias, V., Yospin, G.I., Whitlock, C., 2015. Reconstruction of fire regimes through
1237 integrated paleoecological proxy data and ecological modeling. Frontiers in plant
1238 science, 5, 785.

1239 Ivy-Ochs, S., Kerschner, H., Reuther, A., Preusser, F., Heine, K., Maisch, M., Kubik, P.W.,
1240 Schlüchter, C., 2008. Chronology of the last glacial cycle in the European Alps. Journal of
1241 Quaternary Science 23, 559–573.

1242 Ivy-Ochs, S., Lucchesi, S., Baggio, P., Fioraso, G., Gianotti, G., Monegato, G., Graf, A.A.,
1243 Akscar, N., Christl, M., Carraro, F., Forno, M.G., Schlüchter, C., 2018. New
1244 geomorphological and chronological constraints for glacial deposits in the Rivoli-Avigliana
1245 end-moraine system and the lower Susa Valley (Western Alps, NW Italy). Journal of
1246 Quaternary Science 33, 550–562.

1247 Jobbagy, E.G., Jackson, R.B., 2000. Global controls of forest line elevation in the northern
1248 and southern hemispheres. Global Ecology and Biogeography, 9 (3), 253-268.

1249 Jorda, M., Rosique, T., Evin, J., 2000. Données nouvelles sur l'age du dernier maximum
1250 glaciaire dans les Alpes méridionales françaises. Comptes Rendus de l'Académie des
1251 Sciences - Series IIA - Earth and Planetary Science 331, 187–193.

1252 Kelly, M.A., Kubik, P.W., Von Blanckenburg, F., Schlüchter, C., 2004. Surface exposure
1253 dating of the Great Aletsch Glacier Egesen moraine system, western Swiss Alps, using the
1254 cosmogenic nuclide 10Be. Journal of Quaternary Science, 19 (5), 431-441.

1255 Kindler, P., Guillevic, M., Baumgartner, M., Schwander, J., Landais, A., Leuenberger, M.,
1256 2014. Temperature reconstruction from 10 to 120 kyr b2k from the NGRIP ice core.
1257 Climate of the Past, 10 (2), 887-902.

1258 Körner, C., Paulsen, J., 2004. A world-wide study of high-altitude treeline temperatures. J.
1259 Biogeogr. 31 (5), 713-732.

1260 Kuhlemann, J., Rohling, E.J., Krumrei, I., Kubik, P., Ivy-Ochs, S., Kucera, M., 2008.
1261 Regional Synthesis of Mediterranean atmospheric circulation during the Last Glacial
1262 Maximum. Science, 321(5894), 1338-1340.

1263 Kuhlemann, J., Milivojevic, M., Krumrei, I., Kubik, P.W., 2009. Last glaciation of the Sara
1264 Range (Balkan Peninsula): increasing dryness from the LGM to the Holocene. Austrian
1265 Journal of Earth Sciences, 102, 146–158.

1266 Kuhn, S.L., Stiner, M.C., Güleç, E., Özer, I., Yilmaz, H., Baykara, I., Açikkol, A., Goldberg,
1267 P., Molina, K.M., Ünay, E., Suata-Alpaslan, F., 2009. The early Upper Paleolithic
1268 occupations at Üçağızlı Cave (Hatay, Turkey). Journal of Human Evolution, 56 (2), 87-113.

1269 Kukla, G.J., 1975. Loess stratigraphy of Central Europe. In: Butzer, K.W., Isaac, L.I.
1270 (Eds.), After the Australopithecines. Mouton Publishers, The Hague, 99–187.

1271 Lambeck, K., Purcell, A., Zhao, J., Svensson, N.-O., 2010. The Scandinavian Ice Sheet:
1272 from MIS 4 to the end of the Last Glacial Maximum. Boreas, 39, 410-435.

1273 Lambeck, K., Rouby, H., Purcell, A., Sun, Y., Sambridge, M., 2014. Sea level and global
1274 ice volumes from the Last Glacial Maximum to the Holocene. PNAS, 111(43), 15296-
1275 15303.

61

1276   Lehmkuhl, F., Bösken, J., Hošek, J., Sprafke, T., Marković, S.B., Obreht, I., Hambach, U.,

1277   Sümegi, P., Thiemann, A., Steffens, S., Lindner, H., Veres, D., Zeeden, C., 2018a. Loess

1278   distribution and related Quaternary sediments in the Carpathian Basin. Journal of Maps,

1279   14, 673–682.

1280   Lehmkuhl, F., Pötter, S., Pauligk, A., Bösken, J., 2018b. Loess and other Quaternary

1281   sediments in Germany. Journal of Maps, 14, 330–340.

1282   Leonardi, P., Broglio, A., 1966. Datazione assoluta di un'industria musteriana della grotta

1283   del Broion. Rivista di Scienze Preistoriche 21, (2), 397-405.

1284   Leroy, S.A.G., Giralt, S., Francus, P., Seret, G., 1996. The high sensitivity of the

1285   palynological record in the Vico maar lacustrine sequence (Latium, Italy) highlights the

1286   climatic gradient through Europe for the last 90 ka. Quaternary Science Reviews, 15 (2-3),

1287   189-201.

1288   Lézine, A. M., Von Grafenstein, U., Andersen, N., Belmecheri, S., Bordon, A., Caron, B.,

1289   Cazet, J.-P., Erlenkeuser, H., Fouache, E., Grenier, C., Huntsman-Mapila, P., Hureau-

1290   Mazaudier, D., Manelli, D., Mazaud, A., Robert C., Sulpizio, R., Tiercelin, J.-J., Zanchetta,

1291   G., Zeqollari, Z., 2010. Lake Ohrid, Albania, provides an exceptional multi-proxy record of

1292   environmental changes during the last glacial–interglacial cycle. Palaeogeography,

1293   Palaeoclimatology, Palaeoecology, 287 (1-4), 116-127.

1294   Lindner, H., Lehmkuhl, F., Zeeden, C., 2017. Spatial loess distribution in the eastern

1295   Carpathian Basin: a novel approach based on geoscientific maps and data. Journal of

1296   Maps, 13, 173–181.

1297   Lisiecki, L.E., Raymo, M.E., 2005. A Pliocene-Pleistocene stack of 57 globally distributed

1298   benthic $\delta^{18}O$ records. Paleoceanography, 20 (1).

1299   Lowe, J., Barton, N., Blockley, S., Ramsey, C.B., Cullen, V.L., Davies, W., Gamble, C.,

1300   Grant, K., Hardiman, M., Housley, R., Lane, C.S., Lee, S., Lewis, M., MacLeod, A.,

1301 Menzies, M., Müller, W., Pollard, M., Price, C., Roberts A.P., Rohling, E.J., Satow, C.,

1302 Smith, V.C., Stringer, C.B., Tomlinson, E.L., White, D., Albert, P., Arienzo, I., Barker, G.,

1303 Borić, D., Carandente, A., Civetta, L., Ferrier, C., Guadelli, J.-L, Karkanas, P.,

1304 Koumouzelis, M., Müller, U.C., Orsi, G., Pross, J., Rosi, M., Shalamanov-Korobar, L.,

1305 Sirakov, N, Tzedakis, P.C., 2012. Volcanic ash layers illuminate the resilience of

1306 Neanderthals and early modern humans to natural hazards. Proceedings of the National

1307 Academy of Sciences, 109, 13532–13537.

1308 Magri, D., 1994. Late-Quaternary changes of plant biomass as recorded by pollen-

1309 stratigraphical data: a discussion of the problem at Valle di Castiglione, Italy. Review of

1310 Palaeobotany and Palynology, 81 (2-4), 313-325.

1311 Magri, D., 2008. Two long micro-charcoal records from central Italy. Proceedings of the

1312 Third International Meeting of Anthracology, BAR International Series, 1807, 167-175.

1313 Magri, D., Sadori, L., 1999. Late Pleistocene and Holocene pollen stratigraphy at Lago di

1314 Vico, central Italy. Vegetation History and Archaeobotany, 8 (4), 247-260.

1315 Magri, D., 1999. Late Quaternary vegetation history at Lagaccione near Lago di Bolsena

1316 (central Italy). Review of Palaeobotany and Palynology, 106 (3-4), 171-208.

1317 Makos, M., Rinterknecht, V., Braucher, R., Toloczko-Pasek, A., ASTER Team, 2018. Last

1318 Glacial Maximum and Lateglacial in the Polish High Tatra Mountains - Revised

1319 deglaciation chronology based on the ^{10}Be exposure age dating. Quat. Sc. Rev. 187, 130-

1320 156.

1321 Mangerud, J., Gulliksen, S., Larsen, E., 2010. ^{14}C-dated fluctuations of the western flank of

1322 the Scandinavian Ice Sheet 45–25 kyr BP compared with Bølling–Younger Dryas

1323 fluctuations and Dansgaard–Oeschger events in Greenland. Boreas, 39 (2), 328-342.

1324 Marcott, S.A., Clark, P. U., Padman, L., Klinkhammer, G.P., Springer, S. R., Liu, Z., Otto-

1325 Bliesner, B. L., Carlson, A. E., Ungerer, A., Padman, J., He, F., Cheng J., Schmittner, A.,

63

1326 2011. Ice-shelf collapse from subsurface warming as a trigger for Heinrich events.
1327 Proceedings of the National Academy of Sciences, 108 (33), 13415-13419.

1328 Marciani, G, Ronchitelli, A., Arrighi, S., Badino, F., Bortolini, E., P., Boscato, Boschin, F.,
1329 Crezzini, J., Delpiano, D., Falcucci., A., Figus, C., Lugli, F., Negrino, F., Oxilia G.,
1330 Romandini, M., Riel-Salvatore, J., Spinapolice, E. E., Peresani, M., Moroni, A., Benazzi,
1331 S., this issue. Lithic techno-complexes in Italy from 50 to 39 thousand years BP: an
1332 overview of cultural and technological changes across the Middle-Upper Palaeolithic
1333 boundary.

1334 Margari, V., Gibbard, P.L., Bryant, C.L., Tzedakis, P.C., 2009. Character of vegetational
1335 and environmental changes in southern Europe during the last glacial period; evidence
1336 from Lesvos Island, Greece. Quaternary Science Reviews, 28 (13-14), 1317-1339.

1337 Margherita, C., Oxilia, G., Barbi, V., Panetta, D., Hublin, J-J., Lordkipanidze, D.,
1338 Meshveliani, T., Jakeli, N., Matskevich Z., Bar-Yosef, O., Belfer-Cohen, A., Pinhasi, R.,
1339 Benazzi, S., 2017. Morphological description and morphometric analyses of the Upper
1340 Palaeolithic human remains from Dzudzuana and Satsurblia caves, western
1341 Georgia. Journal of human evolution, 113, 83-90.

1342 Mariani, G.S., Cremaschi, M., Zerboni, A., Zuccoli, L., Trombino, L., 2018.
1343 Geomorphological map of the Mt. Cusna Ridge (Northern Apennines, Italy): evolution of a
1344 Holocene landscape. Journal of Maps 14, 392–401.

1345 Marković, S.B., Stevens, T., Kukla, G.J., Hambach, U., Fitzsimmons, K.E., Gibbard, P.,
1346 Buggle, B., Zech, M., Guo, Z., Hao, Q., Wu, H., O'Hara Dhand, K., Smalley, I.J., Újvári, G.,
1347 Sümegi, P., Timar-Gabor, A., Veres, D., Sirocko, F., Vasiljević, D.A., Jary, Z., Svensson,
1348 A., Jović, V., Lehmkuhl, F., Kovács, J., Svirčev, Z., 2015. Danube loess stratigraphy -
1349 Towards a pan-European loess stratigraphic model. Earth-Science Reviews, 148, 228–
1350 258.

1351 Marti, A., Folch, A., Costa, A., Engwell, S., 2016. Reconstructing the plinian and co-
1352 ignimbrite sources of large volcanic eruptions: A novel approach for the Campanian
1353 Ignimbrite. Scientific reports, 6, 21220.

1354 Martrat, B., Grimalt, J.O., Shackleton, N.J., de Abreu, L., Hutterli, M.A., Stocker, T.F.,
1355 2007. Four climate cycles of recurring deep and surface water destabilizations on the
1356 Iberian margin. Science, 317 (5837), 502-507.

1357 Maselli, V., Trincardi, F., Asioli, A., Ceregato, A., Rizzetto, F., Taviani, M., 2014. Delta
1358 growth and river valleys: the influence of climate and sea level changes on the South
1359 Adriatic shelf (Mediterranean Sea). Quaternary Science Reviews, 99, 146-163.

1360 McDermott, F., 2004. Palaeo-climate reconstruction from stable isotope variations in
1361 speleothems: a review. Quaternary Science Reviews, 23 (7-8), 901-918.

1362 McManus, J.F., Oppo, D.W., Cullen, J.L., 1999. A 0.5-million-year record of millennial
1363 scale climate variability in the North Atlantic. Science, 283 (5404), 971-975.

1364 Mellars, P., 2006. Archeology and the dispersal of modern humans in Europe:
1365 Deconstructing the "Aurignacian". Evolutionary Anthropology: Issues, News, and Reviews:
1366 Issues, News, and Reviews, 15 (5), 167-182.

1367 Mihailović, D., Whallon, R., 2017. Crvena Stijena revisited: the late Mousterian
1368 assemblages. Quaternary International, 450, 36-49.

1369 Miko, S., Ilijanić, N., Hasan, O., Razum, I., Durn, T., Brunović, D., Papatheodorou, G.,
1370 Bakrač, K., Hajek, Tadesse, V., Šparica Miko, M., Crmarić, R., 2017. Submerged karst
1371 landscapes of the Eastern Adriatic. In 5th Regional Scientific Meeting on Quaternary
1372 Geology Dedicated to Geohazards and Final conference of the LoLADRIA project
1373 "Submerged Pleistocene landscapes of the Adriatic Sea".

1374   Moine, O., Antoine, P., Hatté, C., Landais, A., Mathieu, J., Prud'homme, C., Rousseau, D.-
1375   D., 2017. The impact of Last Glacial climate variability in west-European loess revealed by
1376   radiocarbon dating of fossil earthworm granules. PNAS, 114 (24), 6209-6214.

1377   Monegato, G., Ravazzi, C., Donegana, M., Pini, R., Calderoni, G., Wick, L., 2007.
1378   Evidence of a two-fold glacial advance during the last glacial maximum in the Tagliamento
1379   end moraine system (eastern Alps). Quaternary Research 68, 284–302.

1380   Monegato, G., 2012. Local glaciers in the Julian Prealps (NE Italy) during the Last Glacial
1381   Maximum. Alpine and Mediterranean Quaternary. 25 pp. 5–14.

1382   Monegato, G., Scardia, G., Hajdas, I., Rizzini, F., Piccin, A., 2017. The Alpine LGM in the
1383   boreal ice-sheets game. Scientific Reports, 7: 2078.

1384   Moreno, A., Stoll, H., Jiménez-Sánchez, M., Cacho, I., Valero-Garcés, B., Ito, E., Edwards,
1385   R.L., 2010. A speleothem record of glacial (25–11.6 kyr BP) rapid climatic changes from
1386   northern Iberian Peninsula. Global and Planetary Change, 71 (3-4), 218-231.

1387   Morley, M.W., Woodward, J.C., 2011. The Campanian Ignimbrite at Crvena Stijena
1388   rockshelter in Montenegro, Quaternary Research, 75, 683-696.

1389   Moroni, A., Boscato, P., Ronchitelli, A., 2013. What roots for the Uluzzian? Modern
1390   behaviour in Central-Southern Italy and hypotheses on AMH dispersal routes. Quaternary
1391   International, 316, 27-44.

1392   Moroni, A., Ronchitelli, A., Arrighi, S., Aureli, D., Bailey, Boscato, P., Boschin, F.,
1393   Capecchi, G., Crezzini, J., Douka, K., Marciani, G., Panetta, D., Ranaldo, F., Ricci, S.,
1394   Scaramucci, S., Spagnolo, V., Benazzi, S., Gambassini, P., 2018. Grotta del Cavallo
1395   (Apulia–Southern Italy). The Uluzzian in the mirror. Journal of Anthropological
1396   Sciences, 96, 1-36.

1397 Moseley, G. E., Spötl, C., Svensson, A., Cheng, H., Brandstätter, S., Edwards, R. L., 2014.
1398 Multi-speleothem record reveals tightly coupled climate between central Europe and
1399 Greenland during Marine Isotope Stage 3. Geology, 42 (12), 1043-1046.

1400 Müller, U.C., Pross, J., Bibus, E., 2003. Vegetation response to rapid climate change in
1401 Central Europe during the past 140,000 yr based on evidence from the Füramoos pollen
1402 record. Quaternary Research, 59 (2), 235-245.

1403 Müller, U.C., Pross, J., Tzedakis, P.C., Gamble, C., Kotthoff, U., Schmiedl, G., Wulf, S.,
1404 Christanis, K., 2011. The role of climate in the spread of modern humans into Europe.
1405 Quaternary Science Reviews, 30 (3-4), 273-279.

1406 Naughton, F., Sánchez Goñi, M.F., Kageyama, M., Bard, E., Duprat, J., Cortijo, E.,
1407 Desprat, S., Malaize´, B., Joly, C., Rostek, F., Turon, J.-L., 2009. Wet to dry climatic trend
1408 in north-western Iberia within Heinrich events. Earth and Planetary Science Letters, 284,
1409 329–342.

1410 NGRIP members: High-resolution record of Northern Hemisphere climate extending into
1411 the last interglacial period, 2004. Nature, 431, 147–151.

1412 Nigst, P. R., Haesaerts, P., Damblon, F., Frank-Fellner, C., Mallol, C., Viola, B.,
1413 Götzingerh, M., Nivena, L., Trnkai, G., Hublin, J. J., 2014. Early modern human settlement
1414 of Europe north of the Alps occurred 43,500 years ago in a cold steppe-type environment.
1415 Proceedings of the National Academy of Sciences, 111(40), 14394-14399.

1416 Obruchev, V.A., 1914. The problem of North African loess. Zemlevedenie, 4, 26–31 (in
1417 Russian).

1418 Oliva, M., Palacios, D., Fernández-Fernández, J.M., Rodríguez-Rodríguez, L., García-
1419 Ruiz, J.M., Andrés, N., Carrasco, R.M., Pedraza, J., Pérez-Alberti, A., Valcárcel, M.,
1420 Hughes, P.D., 2019. Late Quaternary glacial phases in the Iberian Peninsula. Earth Sc.
1421 Rev. 192, 564-600.

67

1422 Pailler, D., Bard, E., 2002. High frequency palaeoceanographic changes during the past
1423 140000 yr recorded by the organic matter in sediments of the Iberian Margin.
1424 Palaeogeography, Palaeoclimatology, Palaeoecology, 181 (4), 431-452.

1425 Pallàs, R., Rodés, A., Braucher, R., Bourlès, D., Delmas, M., Calvet, M., Gunnell, Y., 2010.
1426 Small isolated glacial catchments as priority targets for cosmogenic surface exposure
1427 dating of Pleistocene climate fluctuations, southeastern Pyrenees. Geology 38, 891–894.

1428 Palma di Cesnola, A., 1989. L'Uluzzien: faciès italien du Leptolithique archaïque.
1429 L'Anthropologie, 93 (4), 783-812.

1430 Palma di Cesnola, A., 2004. Paglicci. L'Aurignaziano e il Gravettiano antico.

1431 Panagiotopoulos, K., Böhm, A., Leng, M.J., Wagner, B., Schäbitz, F., 2014. Climate
1432 variability over the last 92 ka in SW Balkans from analysis of sediments from Lake Prespa.
1433 Climate of the Past, 10 (2), 643-660.

1434 Pellegrini, C., Maselli, V., Cattaneo, A., Piva, A., Ceregato, A., Trincardi, F., 2015.
1435 Anatomy of a compound delta from the post-glacial transgressive record in the Adriatic
1436 Sea. Marine Geology, 362, 43-59.

1437 Peresani, M., Cremaschi, M., Ferraro, F., Falgueres, C., Bahain, J.J., Gruppioni, G.,
1438 Sibilia, E., Quarta G., Calcagnile, L., Dolo, J. M., 2008. Age of the final Middle Palaeolithic
1439 and Uluzzian levels at Fumane Cave, Northern Italy, using 14C, ESR, 234U/230Th and
1440 thermoluminescence methods. Journal of Archaeological Science, 35 (11), 2986-2996.

1441 Peresani, M., 2011. The end of the Middle Palaeolithic in the Italian Alps. An overview on
1442 Neandertal land-use, subsistence and technology. In: Conards N. & Richter J. (eds.),
1443 Neanderthal lifeways, subsistence and technology. One Hundred Fifty Years of
1444 Neanderthal Study. Vertebrate Paleobiology and Paleoanthropology Series, Springer ed.,
1445 249-259.

1446   Peresani, M., 2014. L'Uluzzien en Italie. In: Otte, M. (Ed.), Néandertal/Cro-Magnon. La
1447   Rencontre. Editions Errance, Arles, 61-80.

1448   Peresani, M., Cristiani, E., Romandini, M., 2016. The Uluzzian technology of Grotta di
1449   Fumane and its implication for reconstructing cultural dynamics in the Middle–Upper
1450   Palaeolithic transition of Western Eurasia. Journal of human evolution, 91, 36-56.

1451   Peresani, M., Bertola, S., Delpiano, D., Benazzi, S., Romandini, M., 2018. The Uluzzian in
1452   the north of Italy: insights around the new evidence at Riparo Broion. Archaeological and
1453   Anthropological Sciences, 1-34.

1454   Peresani, M., Bertola, S., Delpiano, D., Benazzi, S., Romandini, M., 2019. The Uluzzian in
1455   the north of Italy: insights around the new evidence at Riparo Broion. Archaeological and
1456   Anthropological Sciences, 11, 3503-3536.

1457   Peters, C., Walden, J., Austin, W.E., 2008. Magnetic signature of European margin
1458   sediments: Provenance of ice-rafted debris and the climatic response of the British ice
1459   sheet during Marine Isotope Stages 2 and 3. Journal of Geophysical Research: Earth
1460   Surface, 113 (F3).

1461   Petersen, S.V., Schrag, D.P., Clark, P.U., 2013. A new mechanism for
1462   Dansgaard-Oeschger cycles. Paleoceanography, 28 (1), 24-30.

1463   Peterson, L.C., Haug, G.H., 2006. Variability in the mean latitude of the Atlantic
1464   Intertropical Convergence Zone as recorded by riverine input of sediments to the Cariaco
1465   Basin (Venezuela). Palaeogeography, Palaeoclimatology, Palaeoecology, 234 (1), 97-113.

1466   Pini, R., Ravazzi, C., Donegana, M., 2009. Pollen stratigraphy, vegetation and climate
1467   history of the last 215 ka in the Azzano Decimo core (plain of Friuli, north-eastern Italy).
1468   Quaternary Science Reviews, 28, 1268-1290.

1469 Pini, R., Ravazzi, C., Reimer P.J., 2010. The vegetation and climate history of the last

1470 glacial cycle in a new pollen record from Lake Fimon (southern Alpine foreland, N-Italy).

1471 Quaternary Science Reviews, 29: 3115-3137.

1472 Popescu, R., Urdea, P., Vespremeanu-Stroe, A., 2017. Deglaciation History of High

1473 Massifs from the Romanian Carpathians: Towards an Integrated View. In: M. Rădoane

1474 and A. Vespremeanu-Stroe (eds.), Landform Dynamics and Evolution in Romania,

1475 Springer Geography, 87-116.

1476 Pross, J., Koutsodendris, A., Christanis, K., Fischer, T., Fletcher, W.J., Hardiman, M.,

1477 Kalaitzidis, S., Knipping, M., Kotthoff, U., Milner, A.M., Müller, U.C., Schmiedl, G.,

1478 Siavalas, G., Tzedakis, P.C., Wulf, S., 2015. The 1.35-Ma-long terrestrial climate archive

1479 of Tenaghi Philippon, northeastern Greece: Evolution, exploration, and perspectives for

1480 future research. Newsletters on Stratigraphy, 48 (3), 253-276.

1481 Pye, K., 1995. The nature, origin and accumulation of loess. Quaternary Science Reviews,

1482 14, 653–667.

1483 Pyle, D.M., Ricketts, G.D., Margari, V., van Andel, T.H., Sinitsyn, A.A., Praslov, N.D.,

1484 Lisitsyn, S., 2006. Wide dispersal and deposition of distal tephra during the Pleistocene

1485 'Campanian Ignimbrite/Y5' eruption, Italy. Quaternary Science Reviews, 25, 2713–2728.

1486 Rasmussen, S.O., Andersen, K.K., Svensson, A.M., Steffensen, J.P., Vinther, B.M.,

1487 Clausen, H.B., Siggaard-Andersen, M.-L., Johnsen S. J., Larsen, L. B., Dahl-Jensen, D.,

1488 Bigler, M., Röthlisberger, R., Fischer, H., Goto-Azuma K., Hansson, M.E., Ruth, U., 2006.

1489 A new Greenland ice core chronology for the last glacial termination. Journal of

1490 Geophysical Research: Atmospheres, 111 (D6).

1491 Rasmussen, S.O., Bigler, M., Blockley, S.P., Blunier, T., Buchardt, S.L., Clausen, H.B.,

1492 Cvijanovic, I., Dahl-Jensen, D., Johnsen, S.J., Fischer, H., 2014. A stratigraphic framework

1493 for abrupt climatic changes during the Last Glacial period based on three synchronized

1494 Greenland ice-core records: refining and extending the INTIMATE event stratigraphy.
1495 Quaternary Science Reviews, 106, 14-28.

1496 Ravazzi, C., Peresani, M., Pini, R., Vescovi, E., 2007. Il Tardoglaciale nelle Alpi italiane e
1497 in Pianura Padana. Evoluzione stratigrafica, storia della vegetazione e del popolamento
1498 antropico. Il Quaternario, 20 (2), 163-184.

1499 Ravazzi, C., Badino, F., Marsetti, D., Patera, G., Reimer, P., 2012. Glacial to paraglacial
1500 history and forest recovery in the Oglio glacier system (Italian Alps) between 26 and 15 ka
1501 cal BP. Quaternary Science Reviews, 58, 146–161.

1502 Reber, R., Akçar, N., Ivy-Ochs, S., Tikhomirov, D., Burkhalter, R., Zahno, C., Lüthold, A.,
1503 Kubik, P.W., Vockenhuber, C., Schlüchter, C., 2014. Timing of retreat of the Reuss glacier
1504 (Switzerland) at the end of the last glacial maximum. Swiss Journal of Geosciences 107,
1505 293–307.

1506 Reille, M., Beaulieu, J.L. de, 1990. Pollen analysis of a long upper Pleistocene continental
1507 sequence in a Velay maar (Massif Central, France). Palaeogeography, Palaeoclimatology,
1508 Palaeoecology, 80 (1), 35-48.

1509 Rey-Rodríguez, I., López-García, J.M., Bennasar, M., Bañuls-Cardona, S., Blain, H.A.,
1510 Blanco-Lapaz, Á., Rodríguez-Álvarez, X.-P., de Lombera-Hermida, A., Díaz-Rodríguez,
1511 M., Ameijenda-Iglesias, A., Agustí, J., Fábregas-Valcarce, R., 2016. Last Neanderthals
1512 and first Anatomically Modern Humans in the NW Iberian Peninsula: Climatic and
1513 environmental conditions inferred from the Cova Eirós small-vertebrate assemblage during
1514 MIS 3. Quaternary Science Reviews 151, 185-197.

1515 Riel-Salvatore, J., Negrino, F., 2018. Human adaptations to climatic change in Liguria
1516 across the Middle–Upper Paleolithic transition. Journal of Quaternary Science, 33 (3), 313-
1517 322.

1518   Roche, D., Paillard, D., Cortijo, E., 2004. Constraints on the duration and freshwater

1519   release of Heinrich event 4 through isotope modelling. Nature, 432 (7015), 379.

1520   Ronchitelli, A., Boscato, P., Gambassini, P., 2009. Gli ultimi Neandertaliani in Italia: aspetti

1521   culturali. In: Facchini, F., Belcastro, G. (Eds.), La lunga storia di Neandertal. Biologia e

1522   comportamento. Jaka Book, Bologna, Italy, 257-288.

1523   Rossato, S., Monegato, G., Mozzi, P., Cucato, M., Gaudioso, B., Miola, A., 2013. Late

1524   Quaternary glaciations and connections to the piedmont plain in the prealpine

1525   environment: the middle and lower Astico Valley (NE Italy). Quat. Int. 288, 8–24.

1526   Rossato, S., Carraro, A., Monegato, G., Mozzi, P., Tateo, F., 2018. Glacial dynamics in

1527   pre-Alpine narrow valleys during the Last Glacial Maximum inferred by lowland fluvial

1528   records (northeast Italy). Earth Surface Dynamics 6, 809-828.

1529   Roucoux, K. H., De Abreu, L., Shackleton, N. J., Tzedakis, P. C., 2005. The response of

1530   NW Iberian vegetation to North Atlantic climate oscillations during the last 65 kyr.

1531   Quaternary Science Reviews, 24(14-15), 1637-1653.

1532   Rousseau, D.-D., Derbyshire, E., Antoine, P., Hatté, C., 2018. European Loess Records.

1533   Reference Module in Earth Systems and Environmental Sciences, 1-17.

1534   Ruddiman, W.F., 1977. Late Quaternary deposition of ice-rafted sand in the subpolar

1535   North Atlantic (lat 40 to 65 N). Geological Society of America Bulletin, 88 (12), 1813-1827.

1536   Ruszkiczay-Rüdiger, Z., Kern, Z., Urdea, P., Braucher, R., Madarász, B.,

1537   Schimmelpfennig, I., 2016. Revised deglaciation history of the Pietrele-Stâni¸soara glacial

1538   complex, Retezat Mts, Southern Carpathians, Romania. Quaternary International, 415,

1539   216–229.

1540   Ruth, U., Bigler, M., Röthlisberger, R., Siggaard-Andersen, M.L., Kipfstuhl, S.,

1541   Goto-Azuma, K., Hansson, M.E., Johnsen, S. J., Lu, H., Steffensen, J.P., 2007. Ice core

1542   evidence for a very tight link between North Atlantic and east Asian glacial climate.
1543   Geophysical Research Letters, 34 (3).

1544   Sadori, L., Koutsodendris, A., Panagiotopoulos, K., Masi, A., Bertini, A., Combourieu-
1545   Nebout, N., Francke, A., Kouli, K., Joannin, S., Mercuri, A.M., Peyron, O., Torri, P.,
1546   Wagner, B., Zanchetta, G., Sinopoli G., Donders, T.H., 2016. Pollen-based
1547   paleoenvironmental and paleoclimatic change at Lake Ohrid (south-eastern Europe)
1548   during the past 500 ka. Biogeosciences, 13 1423-1437.

1549   Salcher, B. C., Starnberger, R., Götz, J., 2015. The last and penultimate glaciation in the
1550   North Alpine Foreland: New stratigraphical and chronological data from the Salzach
1551   glacier. Quat. Int. 388, 218-231.

1552   Sánchez Goñi, M.F., Eynaud, F., Turon, J.L., Shackleton, N.J., 1999. High resolution
1553   palynological record off the Iberian margin: direct land-sea correlation for the Last
1554   Interglacial complex. Earth and Planetary Science Letters, 171 (1), 123-137.

1555   Sánchez Goñi, M.F., Turon, J.L., Eynaud, F., Gendreau, S., 2000. European climatic
1556   response to millennial-scale changes in the atmosphere–ocean system during the Last
1557   Glacial period. Quaternary Research, 54 (3), 394-403.

1558   Sánchez Goñi, M.F., Cacho, I., Turon, J., Guiot, J., Sierro, F., Peypouquet, J., Grimalt, J.,
1559   Shackleton, N., 2002. Synchroneity between marine and terrestrial responses to millennial
1560   scale climatic variability during the last glacial period in the Mediterranean region. Climate
1561   Dynamics, 19 (1), 95-105.

1562   Sánchez Goñi, M.F., Landais, A., Fletcher, W.J., Naughton, F., Desprat, S., Duprat, J.,
1563   2008. Contrasting impacts of Dansgaard–Oeschger events over a western European
1564   latitudinal transect modulated by orbital parameters. Quaternary Science Reviews, 27 (11),
1565   1136-1151.

1566 Sánchez Goñi, M.F., Landais, A., Cacho, I., Duprat, J., Rossignol, L., 2009. Contrasting
1567 intrainterstadial climatic evolution between high and middle North Atlantic latitudes: A
1568 close-up of Greenland Interstadials 8 and 12. Geochemistry, Geophysics, Geosystems, 10
1569 (4).

1570 Satow, C., Tomlinson, E.L., Grant, K.M., Albert, P.G., Smith, V.C., Manning, C.J., Ottolini,
1571 L., Wulf, S., Rohling, E.J., Lowe, J.J., Blockley, S.P.E., Menzies, M.A., 2015. A new
1572 contribution to the Late Quaternary tephrostratigraphy of the Mediterranean: Aegean Sea
1573 core LC21. Quaternary Science Reviews, 117, 96-112.

1574 Schneider, U., Becker, A., Finger, P., Meyer-Christoffer, A., Ziese, M., Rudolf, B., 2014.
1575 GPCC's new land surface precipitation climatology based on quality-controlled in situ data
1576 and its role in quantifying the global water cycle, Theoretical and Applied Climatology, 115,
1577 1–15.

1578 Seguinot, J., Ivy-Ochs, S., Jouvet, G., Huss, M., Funk, M., Preusser, F., 2018. Modelling
1579 last glacial cycle ice dynamics in the Alps. The Cryosphere, 12, 3265-3285.

1580 Seierstad, I.K., Abbott, P.M., Bigler, M., Blunier, T., Bourne, A.J., Brook, E., Buchardt, S.,
1581 L., Buizert, C., Clausen, H.B., Cook E., Dahl-Jensen, D., Davies, S.M., Guillevic, M.,
1582 Johnsen, S.J., Pedersen, D.S., Popp, T.J., Rasmussen, S.O., Severinghaus, J.P.,
1583 Svensson, A., Vinther, B.M., 2014. Consistently dated records from the Greenland GRIP,
1584 GISP2 and NGRIP ice cores for the past 104 ka reveal regional millennial-scale δ^{18}O
1585 gradients with possible Heinrich event imprint. Quaternary Science Reviews, 106, 29-46.

1586 Seret, G., Dricot, E., Wansard, G. 1990. Evidence for an early glacial maximum in the
1587 French Vosges during the last glacial cycle. Nature 346, 453-456.

1588 Serrano, E., Gómez-Lende, M., González-Amuchastegui, M.J., González-García, M.,
1589 González-Trueba, J.J., Pellitero, R., Rico, I., 2015. Glacial chronology, environmental
1590 changes and implications for human occupation during the upper Pleistocene in the
1591 eastern Cantabrian Mountains. Quaternary International 364, 22–34.

74

1592 Sirocko, F., Knapp, H., Dreher, F., Förster, M.W., Albert, J., Brunck, H., Veres, D., Dietrich,
1593 S., Zech, M., Hambach, U., Röhner, M., Rudert, S., Schwibus, K., Adams, C., Sigl, P.,
1594 2016. The ELSA-Vegetation-Stack: Reconstruction of Landscape Evolution Zones (LEZ)
1595 from laminated Eifel maar sediments of the last 60,000 years. Global and Planetary
1596 Change, 142, 108-135.

1597 Smalley, I.J., Leach, J.A., 1978. The origin and distribution of the loess in the Danube
1598 basin and associated regions of East-Central Europe e a review. Sedimentary Geology,
1599 21, 1–26.

1600 Spennato, A.G., 1981. I livelli protoaurignaziani della Grotta di Serra Cicora. Studi per
1601 l'Ecologia del Quaternario 61, 52–76.

1602 Spötl, C., Mangini, A., Frank N., Eichstädter, R., Burns, S.J., 2002. Start of the Last
1603 Interglacial period at 135 ka: evidence from a high alpine speleothem. Geology 30 (9),
1604 815-818.

1605 Spötl, C., Mangini, A., 2007. Speleothems and paleoglaciers. Earth and Planetary Science
1606 Letters, 254 (3-4), 323-331.

1607 Staff, R. A., Hardiman, M., Ramsey, C. B., Adolphi, F., Hare, V. J., Koutsodendris, A.,
1608 Pross, J., 2019. Reconciling the Greenland ice-core and radiocarbon timescales through
1609 the Laschamp geomagnetic excursion. Earth and Planetary Science Letters, 520, 1-9.

1610 Starkovich, B.M., 2017. Paleolithic subsistence strategies and changes in site use at
1611 Klissoura Cave 1 (Peloponnese, Greece). Journal of human evolution, 111, 63-84.

1612 Staubwasser, M., Drăgușin, V., Onac, B.P., Assonov, S., Ersek, V., Hoffmann, D.L., Veres,
1613 D., 2018. Impact of climate change on the transition of Neanderthals to modern humans in
1614 Europe. Proceedings of the National Academy of Sciences, 115 (37), 9116-9121.

1615   Steegmann Jr., A.T., Cerny, F.J., Holliday, T.W., 2002. Neandertal cold adaptation:
1616   physiological and energetic factors. American Journal of Human Biology, 14 (5), 566-583.

1617   Steffensen, J.P., Andersen, K.K., Bigler, M., Clausen, H. B., Dahl-Jensen, D., Fischer, H.,
1618   Goto-Azuma, K., Hansson M., Johnsen, S.J., Jouzel, J., Masson-Delmotte, V., Popp, T.,
1619   Rasmussen, S.O., Röthlisberger, R., Ruth, U., Stauffer B., Siggaard-Andersen, M.-L.,
1620   Sveinbjörnsdóttir, A., E., Svensson, A., White, J.W.C., 2008. High-resolution Greenland ice
1621   core data show abrupt climate change happens in few years. Science, 321 (5889), 680-
1622   684.

1623   Stern, J.V., Lisiecki, L.E., 2013. North Atlantic circulation and reservoir age changes over
1624   the past 41,000 years. Geophysical Research Letters, 40 (14), 3693-3697.

1625   Stiner, M.C., Kozowski, J.K., Kuhn, S.L., Karkanas, P., Koumouzelis, M., 2007. Klissoura
1626   Cave 1 and the Upper Paleolithic of Southern Greece in Cultural and Ecological Context.
1627   Eurasian Prehistory 7, 309–321.Stoll, H.M., Moreno, A., Mendez-Vicente, A., Gonzalez-
1628   Lemos, S., Jimenez-Gochez, M., Dominguez-Cuesta, M.J., Edwards, R.L., Cheng. H.,
1629   Wang, X., 2013. Paleoclimate and growth rates of speleothems in the northwestern Iberian
1630   Peninsula over the last two glacial cycles. Quaternary Research, 80 (2), 284-290.

1631   Svensson, A., Andersen, K.K., Bigler, M., Clausen, H.B., Dahl-Jensen, D., Davies, S.M.,
1632   Johnsen, S.J., Muscheler, R., Parrenin, F., Rasmussen, S.O., Röthlisberger, R., Seierstad,
1633   I., Steffensen, J.P., Vinther, B.M., 2008. A 60,000 year Greenland stratigraphic ice core
1634   chronology. Climate of the Past, 4, 47–57.

1635   Temovski, M., Madarász, B., Kern, Z., Milevski, I., Ruszkiczay-Rüdiger, Z., 2018. Glacial
1636   Geomorphology and Preliminary Glacier Reconstruction in the Jablanica Mountain,
1637   Macedonia, Central Balkan Peninsula. Geosciences 8, 270.
1638   doi:10.3390/geosciences8070270.

1639   Terhorst, B., Sedov, S., Sprafke, T., Peticzka, R., Meyer-Heintze, S., Kühn, P., Solleiro

1640   Rebolledo, E., 2015. Austrian MIS 3/2 loess–palaeosol records-Key sites along a west–

1641   east transect. Palaeogeography, Palaeoclimatology, Palaeoecology, 418, 43–56.

1642   Thiel, C., Horváth, E., Frechen, M., 2014. Revisiting the loess/palaeosol sequence in Paks,

1643   Hungary: a post-IR IRSL based chronology for the 'Young Loess Series'. Quaternary

1644   International, 319, 88–98

1645   Timar, A., Vandenberghe, D., Panaiotu, E.C., Panaiotu, C.G., Necula, C., Cosma, C., van

1646   den Haute, P., 2010. Optical dating of Romanian loess using fine-grained quartz.

1647   Quaternary Geochronology, 5 (2-3), 143–148.

1648   Timar-Gabor, A., Vandenberghe, D.A.G., Vasiliniuc, S., Panaoitu, C.E., Panaiotu, C.G.,

1649   Dimofte, D., Cosma, C., 2011. Optical dating of Romanian loess: a comparison between

1650   silt-sized and sand-sized quartz. Quaternary International, 240, 62–70.

1651   Tinner, W., Hubschmid, P., Wehrli, M., Ammann, B., Conedera, M., 1999. Long-term forest

1652   fire ecology and dynamics in southern Switzerland. Journal of Ecology, 87, 273-289.

1653   Toucanne, S., Soulet, G., Freslon, N., Jacinto, R.S., Dennielou, B., Zaragosi, S. Eynaud;

1654   F., Bourillet, J.-F., Bayon, Germain., 2015. Millennial-scale fluctuations of the European

1655   Ice Sheet at the end of the last glacial, and their potential impact on global climate.

1656   Quaternary Science Reviews, 123, 113-133.

1657   Tranquillini, W., 1979. General Features of the Upper Timberline. In Physiological Ecology

1658   of the Alpine Timberline. Springer Berlin Heidelberg, 1-4.

1659   Turkish State Meteorological Service, 2006. Climate of Turkey. Turkish State

1660   Meteorological Service. Archived from the original on April 19, 2008. Retrieved 2006-12-

1661   27.

1662 Tzedakis, P. C., 1999. The last climatic cycle at Kopais, central Greece. Journal of the
1663 Geological Society, 156 (2), 425-434.

1664 Tzedakis, P.C., Lawson, I.T., Frogley, M.R., Hewitt, G.M., Preece, R.C., 2002. Buffered
1665 tree population changes in a Quaternary refugium: evolutionary implications. Science, 297
1666 (5589), 2044-2047.

1667 Tzedakis, P. C., Frogley, M. R., Lawson, I. T., Preece, R. C., Cacho, I., De Abreu, L.,
1668 2004. Ecological thresholds and patterns of millennial-scale climate variability: the
1669 response of vegetation in Greece during the last glacial period. Geology, 32 (2), 109-112.

1670 Tzedakis, P.C., Hooghiemstra, H., Pälike, H., 2006. The last 1.35 million years at Tenaghi
1671 Philippon: revised chronostratigraphy and long-term vegetation trends. Quaternary
1672 Science Reviews, 25 (23-24), 3416-3430.

1673 Valen, V., Larsen, E., Mangerud, J.A.N., 1995. High-resolution paleomagnetic correlation
1674 of Middle Weichselian ice-dammed lake sediments in two coastal caves, western
1675 Norway. Boreas, 24 (2), 141-153.

1676 van Andel, T.H., Tzedakis P.C., 1998. Priority and opportunity: reconstructing the
1677 European Middle Palaeolithic climate and landscape. In (Bailey, J., ed.): Science in
1678 Archaeology. An agenda for the future. English Heritage, 37-45.

1679 van Andel, T.H., Davies, W., Weninger, B., 2003. The human presence in Europe during
1680 the last glacial period I: human migrations and the changing climate. Neanderthals and
1681 modern humans in the European landscape during the last glaciation: archaeological
1682 results of the Stage, 3, 31-56.

1683 Van Meerbeeck, C.J., Renssen, H., Roche, D.M., Wohlfarth, B., Bohncke, S.J.P., Bos,
1684 J.A.A., Engels, S., Helmens, K.F., Sánchez Goñi, F., Svensson, A., Vandenberghe J.,
1685 2011. The nature of MIS 3 stadial-interstadial transitions in Europe: new insights from
1686 model-data comparison. Quaternary Science Reviews, 30, 3618-3637.

1687   Verheul, J., Zickel, M., Becker, D., Willmes, C., 2015. LGM major inland waters of Europe-

1688   GIS dataset. CRC806-Database, DOI: http://dx. doi. org/10.5880/SFB806, 14.

1689   Villa, P., Roebroeks, W., 2014. Neandertal demise: An archaeological analysis of the

1690   modern human superiority complex. PLoS ONE, 9(4), e96424.

1691   Wacha, L., Pavlaković, S.M., Frechen, M., Crnjaković, M., 2011a. The Loess chronology of

1692   the Island of Susak, Croatia. E&G Quaternary Science Journal, 60, 153–169.

1693   Wacha, L., Pavlakovic, S., Novothny, A., Crnjaković, M., Frechen, M., 2011b.

1694   Luminescence dating of Upper Pleistocene loess from the Island of Susak in Croatia.

1695   Quaternary International, 234, 50–61.

1696   Waelbroeck, C., Labeyrie, L., Michel, E., Duplessy, J. C., Lambeck. K., McManus, J. F.,

1697   Balbon, E., Labracherie, M., 2002. Sea-level and deep water temperature changes derived

1698   from benthic foraminifera isotopic records. Quaternary Science Reviews, 21, 295-305.

1699   Wainer, K., Genty, D., Blamart, D., Hoffmann, D., Couchoud, I., 2009. A new stage 3

1700   millennial climatic variability record from a SW France speleothem. Palaeogeography,

1701   Palaeoclimatology, Palaeoecology, 271 (1), 130-139.

1702   Walter, H., Breckle, S.W., 1986. Spezielle Ökologie der gemässigten und arktischen

1703   Zonen Euro-Nordasiens: Zonobiom VI-IX. Fischer.

1704   Weber, M., Scholz, D., Schröder-Ritzrau, A., Deininger, M., Spötl, C., Lugli, F., Mertz-

1705   Kraus, R., Jochum, K.P., Fohlmeister, J., Stumpf, C.F., Riechelmann, D.F.C., 2018.

1706   Evidence of warm and humid interstadials in central Europe during early MIS 3 revealed

1707   by a multi-proxy speleothem record. Quaternary Science Reviews, 200, 276-286.

1708   Whitlock, C., Larsen, C., 2001. Charcoal as a fire proxy. Smol, JP, Birks, HJB and Last,

1709   WM (eds.) Tracking environmental change using lake sediments Vol. 3, Terrestrial, algal,

1710   and Siliceous Indicators, 75-97.

1711   Whitlock, C., Larsen, C., 2001. Charcoal as a fire proxy. Smol, JP, Birks, HJB and Last,
1712   WM (eds.) Tracking environmental change using lake sediments Vol. 3, Terrestrial, algal,
1713   and Siliceous Indicators, 75-97.

1714   Wijmstra, T.A., 1969. Palynology of the first 30 metres of a 120 m deep section in northern
1715   Greece. Acta Botanica Neerlandica, 18 (4), 511-527.

1716   Wohlfarth, B., 2010. Ice-free conditions in Sweden during Marine Oxygen Isotope Stage
1717   3?. Boreas, 39 (2), 377-398.

1718   Woillard, G.M., 1978. Grande Pile peat bog: a continuous pollen record for the last
1719   140,000 years. Quaternary Research, 9, 1-21.

1720   Wood, R. E., Douka, K., Boscato, P., Haesaerts, P., Sinitsyn, A., Higham, T., 2012.
1721   Testing the ABOx-SC method: dating known-age charcoals associated with the
1722   Campanian Ignimbrite. Quaternary Geochronology, 9, 16-26.

1723   Wood, R., 2015. From revolution to convention: the past, present and future of radiocarbon
1724   dating. Journal of Archaeological Science, 56, 61-72.

1725   Wroe, S., Parr, W.C., Ledogar, J.A., Bourke, J., Evans, S.P., Fiorenza, L., Benazzi, S.,
1726   Hublin, J.-J., Stringer C., Kullmer, O., Curry, M., Rae, T.C., Yokley, T.R., 2018. Computer
1727   simulations show that Neanderthal facial morphology represents adaptation to cold and
1728   high energy demands, but not heavy biting. Proceedings Royal Society B, 285 (1876),
1729   20180085.

1730   Wulf, S., Hardiman, M. J., Staff, R.A., Koutsodendris, A., Appelt, O., Blockley, S.P., Lowe,
1731   J.J., Manning C.J., Ottolini, L., Schmitt, A.K., Smith, V.C., Tomlinson E.L., Vakhrameeva,
1732   P., Knipping, M., Kotthoff, U., Milner, A.M., Müller, U.C., Christanis K., Kalaitzidis S.,
1733   Tzedakis, P.C., Schmiedl G., Pross J., 2018. The marine isotope stage 1–5 cryptotephra
1734   record of Tenaghi Philippon, Greece: Towards a detailed tephrostratigraphic framework for
1735   the Eastern Mediterranean region. Quaternary Science Reviews, 186, 236-262.

80

1736 Wutke, K., Wulf, S., Tomlinson, E. L., Hardiman, M., Dulski, P., Luterbacher, J., Brauer, A.,
1737 2015. Geochemical properties and environmental impacts of seven Campanian tephra
1738 layers deposited between 40 and 38 ka BP in the varved lake sediments of Lago Grande
1739 di Monticchio, southern Italy. Quaternary Science Reviews, 118, 67-83.

1740 Yazbeck, C., 2004. Le Paleolithique du Liban: bilan critique. Paleorient, 30, 111-126.

1741 Zanchetta, G., Giaccio, B., Bini, M., Sarti, L., 2018. Tephrostratigraphy of Grotta del
1742 Cavallo, Southern Italy: Insights on the chronology of Middle to Upper Palaeolithic
1743 transition in the Mediterranean. Quaternary Science Reviews, 182, 65-77.

1744 Zasadni, J., Klapyta, P., 2014. The Tatra Mountains during the Last Glacial Maximum.
1745 Journal of Maps, 10 (3), 440-456.

1746 Žebre, M., Stepišnik, U., 2014. Reconstruction of Late Pleistocene glaciers on Mount
1747 Lovćen, Montenegro. Quaternary International, 353, 225–235.

1748 Žebre, M., Stepišnik, U., 2015. Glaciokarst geomorphology of the northern Dinaric alps:
1749 Snežnik (Slovenia) and Gorski Kotar (Croatia). Journal of Maps 5, 873-881.
1750 doi.org/10.1080/17445647.2015.1095133.

1751 Žebre, M., Stepišnik, U., Colucci, R.R., Forte, E., Monegato, G., 2016. Evolution of a karst
1752 polje influenced by glaciation: the Gomance piedmont polje (northern Dinaric Alps).
1753 Geomorphology, 257, 143–154.

1754 Žebre, M., Jež, J., Mechernich, S., Mušič, B., Horn, B., Jamšek Rupnik, P., 2019.
1755 Paraglacial adjustment of alluvial fans to the last deglaciation in the Snežnik Mountain,
1756 Dinaric karst (Slovenia). Geomorph. 332, 66-79.

1757 Zerboni, A., Trombino, L., Frigerio, C., Livio, F., Berlusconi, A., Michetti, A.M., Rodnight,
1758 H., Spötl, C., 2015. The loess -paleosol sequence at Monte Netto: a record of climate

change in the Upper Pleistocene of the central Po Plain, northern Italy. Journal of Soils and Sediments, 15, 1329-1350.

Zerboni, A., Amit, R., Baroni, C., Coltorti, M., Ferrario, M.F., Fioraso, G., Forno, M.G., Frigerio, C., Gianotti, F., Irace, A., Livio, F., Mariani, G.S., Michetti, A.M., Monegato, G., Mozzi, P., Orombelli, G., Perego, A., Porat, N., Rellini, I., Trombino, L., Cremaschi, M., 2018. Towards a map of the Upper Pleistocene loess of the Po Plain Loess Basin (Northern Italy). Alpine and Mediterranean Quaternary, 31, 253–256.

Zhornyak, L.V., Zanchetta, G., Drysdale, R. N., Hellstrom, J.C., Isola, I., Regattieri, E., Piccini, L., Baneschi, I., Couchoud, I., 2011. Stratigraphic evidence for a "pluvial phase" between ca 8200–7100 ka from Renella cave (Central Italy). Quaternary Science Reviews, 30 (3-4), 409-417.

Zilhão, J, Bank,s W.E., d'Errico, F., Gioia. P., 2015. Analysis of site formation and assemblage integrity does not support attribution of the Uluzzian to modern humans at Grotta del Cavallo. PLosOne 10(7): e0131181.

Figure captions

Fig. 1 Comparison of Northern Hemisphere terrestrial and marine paleoclimate proxies: (a) NGRIP δ^{18}O record (Rasmussen et al., 2014), (b) temperature reconstruction based on δ^{15}N (Kindler et al., 2014) and (c) calcium ion concentration ([Ca^{2+}]) record (Rasmussen et al 2014), plotted all on the GICC05modelext chronology (Rasmussen et al., 2014); (d) NEEM ^{17}O-excess permeg (Guillevic et al., 2014); (e) δ^{18}O record from Northern Alps (NALPS) speleothems (Moseley et a., 2014) plotted on its timescale; (f) MD95-2042 Sea Surface Temperature record (Darfeuil et al., 2016), (g) *Neogloboquadrina pachyderma*

82

1784 abundance and (h) Ice-Radfted Debris record (Sánchez Goñi et al., 2008), plotted each on

1785 their own timescale. Vertical grey bars indicate Greenland Stadial (GS). Heinrich events

1786 (HEs) are indicated according to MD95-2042 chronology (Sánchez Goñi et al., 2008).

1787

1788 **Fig. 2** European biogeographical map. Overview of mid- to high-resolution marine and

1789 terrestrial records entirely or partially covering MIS 3.

1790

1791 **Fig. 3** Vegetation changes throughout MIS 3 in several high- to mid-resolution terrestrial

1792 pollen records from S-Europe and Mediterranean region. Pollen curves: % of woody taxa

1793 (sum of trees and shrubs) (light green); % of arboreal pollen (dark green); % of xerophytic

1794 elements (sum of *Artemisia* and Chenopodiaceae) (grey). Black histograms show pollen-

1795 slide microcharcoal concentrations. All records are plotted using the latest available

1796 chronology for each individual site. NGRIP $\delta^{18}O$ record is also shown (NGRIP members,

1797 2004; Rasmussen et al., 2014). Red numbers indicate Greenland Interstadials (GI),

1798 modified from Fletcher et al., 2010. Heinrich events (HEs) are indicated according to

1799 MD95-2042 chronology (Sánchez Goñi et al., 2008).

1800

1801 **Fig. 4 - A)** Ecogeography of Greenland Interstadial 12 (GI 12; ca. 46.8 to 44.2 ka

1802 according to Rassmussen et al., 2014), showing reconstructed gradients within European

1803 eco-climatic zones. Digital Elevation Model (base topography – ETOPO 2011;

1804 ETRS_1989_LAEA_152 projected coordinate system). Sea surface lowered to -74 m asl

1805 (Waelbroeck et al., 2002; Antonioli, 2012). Baltic lake drawn after Lambeck et al., 2010.

1806 The mountain glaciers (pale blue) and the main Alpine valley glaciers (cyan triangles) are

1807 inferred both from simulations (Seguinot et al., 2018) and ELA calculations, for more

1808 information see section 4.1.2. Colour scale bars depict eco-climatic zones gradients.

1809 Sharp limits mark reconstructed elevational timberlines position and mountain glaciers

1810 extent in different mountain systems within each eco-climatic zone, see sections 4.1 and

1811 4.2. **B)** Palaeogeographic map of Europe during the Last Glacial Maximum. Digital

1812 Elevation Model (base topography – ETOPO 2011; ETRS_1989_LAEA_152 projected

1813 coordinate system). Sea level drop at – 120 m (Pellegrini et al., 2015; Maselli et al 2014).

1814 Scandinavian and British Islands ice sheets (pale blue) after Hughes et al. (2016) at 22 ka.

1815 The mountain glaciers (pale blue) from Ehlers et al. (2011) with updated reconstructions in

1816 the Tatra Mountains (Zasadni and Klapyta, 2014), Dinarides (Kuhlemann et al., 2009;

1817 Žebre and Stepišnik, 2014, 2015; Temovski et al., 2018), Pyrenees (Delmas, 2015),

1818 Cantabrian range (Serrano et al., 2015). Alpine glaciers downloaded from

1819 https://booksite.elsevier.com/9780444534477/ and modified in the Italian side using

1820 updated reconstructions (Ravazzi et al., 2012; Monegato et al., 2017; Gianotti et al., 2015;

1821 Ivy-Ochs et al., 2018; Rossato et al., 2018). Major European and eastern European lakes

1822 and rivers after Toucanne et al. (2015) and Verheul et al. (2015), Adriatic lakes (Miko et

1823 al., 2017) and rivers simplified from Maselli et al. (2014). Italian rivers draining major ice

1824 lobes at the outlet of alpine valleys are indicated with solid blue lines, outlined lines are

1825 used for lower-order rivers. Aeolian sediments (yellow polygons) based on data from

1826 compilations by Haase et al. (2007); Italian loess from Zerboni et al. (2018).

1827

1828 **Fig. 5** Spatial vegetation changes at fixed 5 ka yrs long time slices between 60 and 30 ka

1829 yrs cal BP. The selected taxa are grouped according to their ecology and climatic

1830 preferences. Eurythermic conifers (orange): sum of *Pinus* and *Juniperus*; Temperate forest

1831 (red): sum of deciduous *Quercus*, *Alnus*, *Fagus*, *Acer*, *Corylus*, *Carpinus*, *Fraxinus*, *Ulmus*,

1832 *Tilia* and *Salix*; Xerophytic taxa (dark blue): sum of *Artemisia* and Chenopodiaceae. Italian

1833 Peninsula sketch map shows sea level 70 m below the present-day coastline (courtesy by

1834 S. Ricci, University of Siena), based on the global sea-level curve by Waelbroeck et al.

1835 (2002), but lacking estimation of post-MIS3 sedimentary thickness and eustatic magnitude.
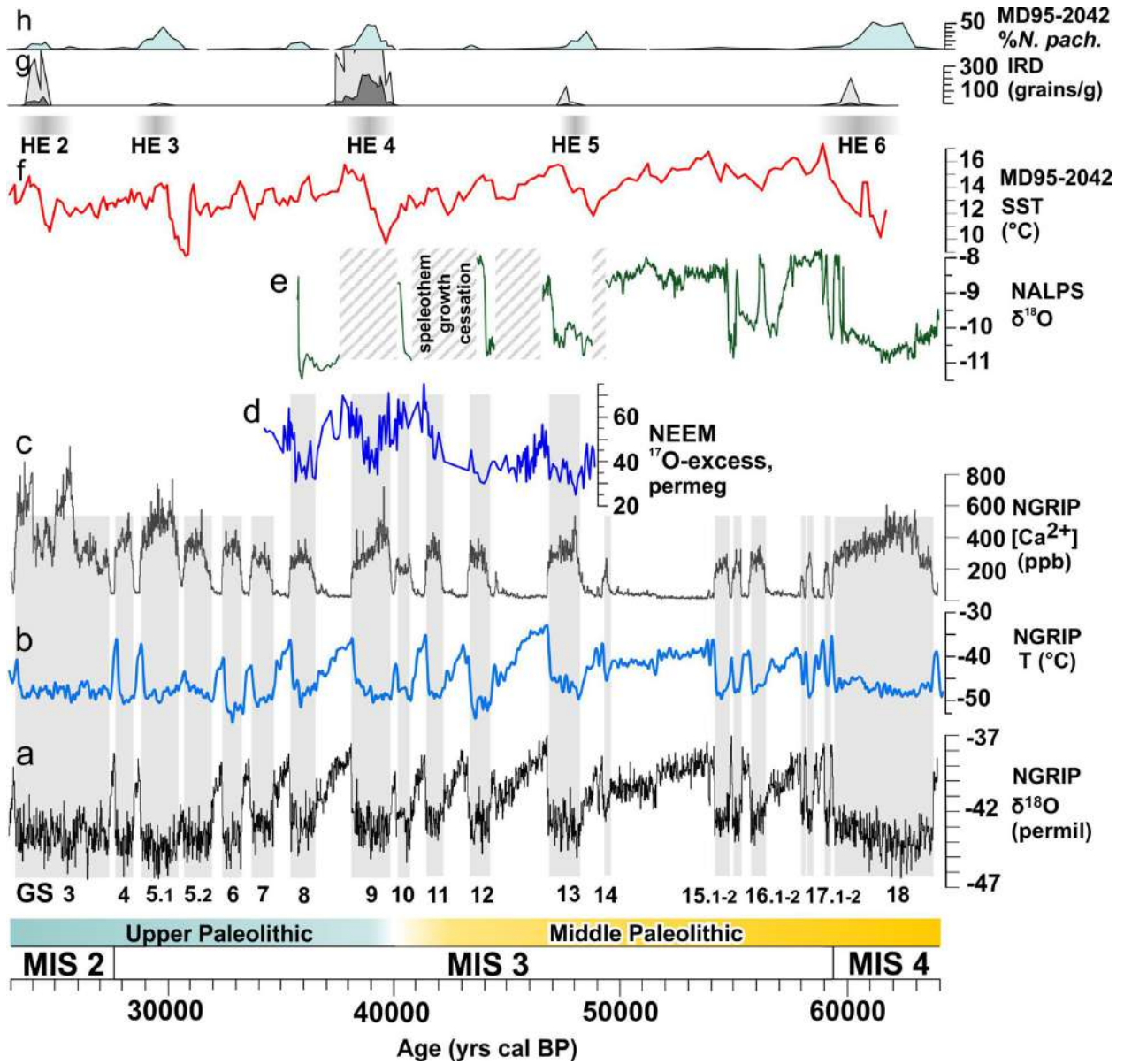
1836

1837 **Fig. 6** Sketch map showing the position of the Palaeolithic sites documenting the Uluzzian

1838 culture: 1) Klissoura Cave (Stiner et al., 2007); 2) Kephalari Cave (Darlas and Psathi,

1839 2016); 3) Crvena Stijena (Morley and Woodward, 2011); 4) Grotta del Cavallo (Moroni et

1840 al., 2018); 5) Grotta di Serra Cicora (Spennato 1981); 6) Grotta Mario Bernardini (Borzatti

1841   von Löwenstern 1970); 7) Grotta di Uluzzo (Borzatti von Löwenstern 1965); 8) Grotta di

1842   Uluzzo C (Borzatti von Löwenstern 1966); 9) Grotta delle Veneri (Cremonesi, 1987); 10)

1843   Torre Testa (Moroni et al., 2018); 11) Falce del Viaggio (Moroni et al., 2018); 12) Foresta

1844   Umbra (Moroni et al., 2018); 13) Atella Basin (Moroni et al., 2018); 14) Castelcivita

1845   (Gambassini, 1997); 15) Grotta della Cala (Benini et al.,1997); 16) S. Pietro a Maida

1846   (Moroni et al., 2018); 17) Tornola (Moroni et al., 2018); 18) Colle Rotondo (Moroni et al.,

1847   2018); 19) Grotta della Fabbrica (Dini 2012); 20) Val Berretta (Moroni et al., 2018); 21)

1848   Poggio Calvello (Moroni et al., 2018); 22) S. Lucia I (Moroni et al., 2018); 23) Indicatore

1849   (Moroni et al., 2018); 24) Villa Ladronaia (Moroni et al., 2018); 25) Maroccone (Moroni et

1850   al., 2018); 26) Salviano (Moroni et al., 2018); 27) Podere Collina (Moroni et al., 2018); 28)

1851   Val di Cava (Moroni et al., 2018); 29) Casa ai Pini (Moroni et al., 2018); 30) San Romano

1852   (Moroni et al., 2018); 31) San Leonardo (Moroni et al., 2018); 32) Porcari (Moroni et al.,

1853   2018); 33) Riparo del Broion (Peresani et al., 2019); 34) Grotta Fumane (Peresani et al.,

1854   2016).

1855

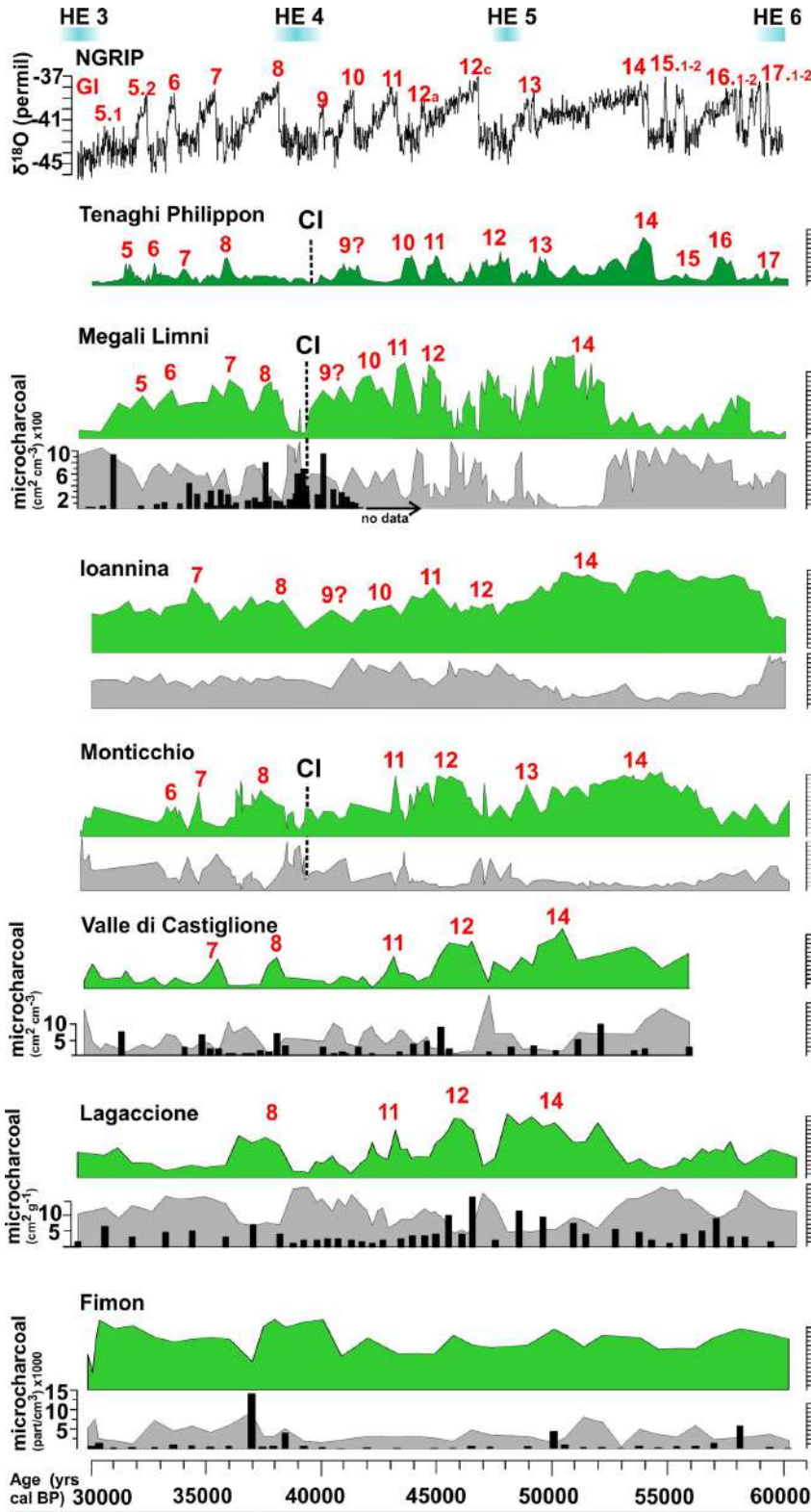1856   **Fig. 7** Geographic distribution of the Campanian Ignimbrite (CI) distal tephra layer in

1857   terrestrial and marine records (red dots) and archaeological sites (yellow squares). On the

1858   right: Tenaghi Philippon paleoecological record showing the CI chronostratigraphic

1859   position. Selected pollen curves of % arboreal pollen (green) and temperate taxa (orange)

1860   between 30 and 60 ka are shown.

1861

h   50 MD95-2042
        %N. pach.
g   300 IRD
     100 (grains/g)

HE 2   HE 3   HE 4   HE 5   HE 6

f   16 MD95-2042
     14 SST
     12 (°C)
     10

e   -8 NALPS
speleothem -9 δ¹⁸O
growth
cessation -10
           -11

d   60 NEEM
     40 ¹⁷O-excess,
        permeg
     20

c   800 NGRIP
     600 [Ca²⁺]
     400 (ppb)
     200

b   -30 NGRIP
     -40 T (°C)
     -50

a   -37 NGRIP
     -42 δ¹⁸O
         (permil)
     -47

GS 3   4 5.1 5.2 6 7 8   9 10 11 12   13 14   15.1-2 16.1-2 17.1-2 18

Upper Paleolithic   Middle Paleolithic

MIS 2   MIS 3   MIS 4

30000   40000   50000   60000

Age (yrs cal BP)

Biogeographical Regions
- Alpine
- Anatolian
- Atlantic
- Black Sea
- Boreal
- Continental
- Mediterranean
- Pannonian
- Steppic
- outside Europe

Terrestial pollen records
Marine pollen/isotopic records
Speleothemes

MIS 3 entirely covered
MIS 3 partially covered

Bunker cave
Eifel maar
Füramoos
La Grand Pile
Hölloch cave
Kleegruben cave
MD 04 2845
Les Eches
Azzano Decimo
Villars cave
Ribains
Fimon
Lagaccione Vico
MD 95 2042
Abric Romani
Ohrid
Tenaghi Philippon
Valle di Castiglione
Prespa
Megali Limni
Monticchio
Ioannina
Kopais
ODP 976
MD 95 2043
LC 21

HE 3   HE 4   HE 5   HE 6

NGRIP

Tenaghi Philippon

Megali Limni

Ioannina

Monticchio

Valle di Castiglione

Lagaccione

Fimon

Age (yrs cal BP)   30000   35000   40000   45000   50000   55000   60000

Woody taxa   Arboreal pollen   Steppe/desert forb-shrub (*Artemisia* + Chenopodiaceae)   CI Campanian Ignimbrite (tephra marker)

Biogeographical regions, physical and climate setting

Mediterranean region (Greece)
Lat.: 41.17˚, Long.: 24.33˚
Altitude: 40 m asl
Present-day climate: Mediterranean; mean T January: 3.4 °C and mean T July: 23.9 ºC; mean annual P: 600 mm

Mediterranean region (Greece, Lesvos island)
Lat.: 39.1˚, Long.: 26.32˚
Altitude: 323 m asl
Present-day climate: Mediterranean with mean T winter: 10.4 °C; T summer: 26.1 °C; mean annual P: 725 mm - 415 mm (East to West)

Mediterranean region (Greece)
Lat.: 39.75˚, Long.: 20.85˚
Altitude: 470 m asl
Present-day climate: sub-Mediterranean with high annual P and moderate summer drought; mean annual P: 1200 mm

Mediterranean region (Italian peninsula)
Lat.: 40.93˚, Long.: 15.62˚
Altitude: 656 m asl
Present-day climate: wet winters with a pronunced dry period in summer; mean annual T: 13.7 °C; mean annual P: 815 mm

Mediterranean region (Italian peninsula)
Lat.: 41.88˚, Long.: 12.77˚
Altitude: 44 m asl
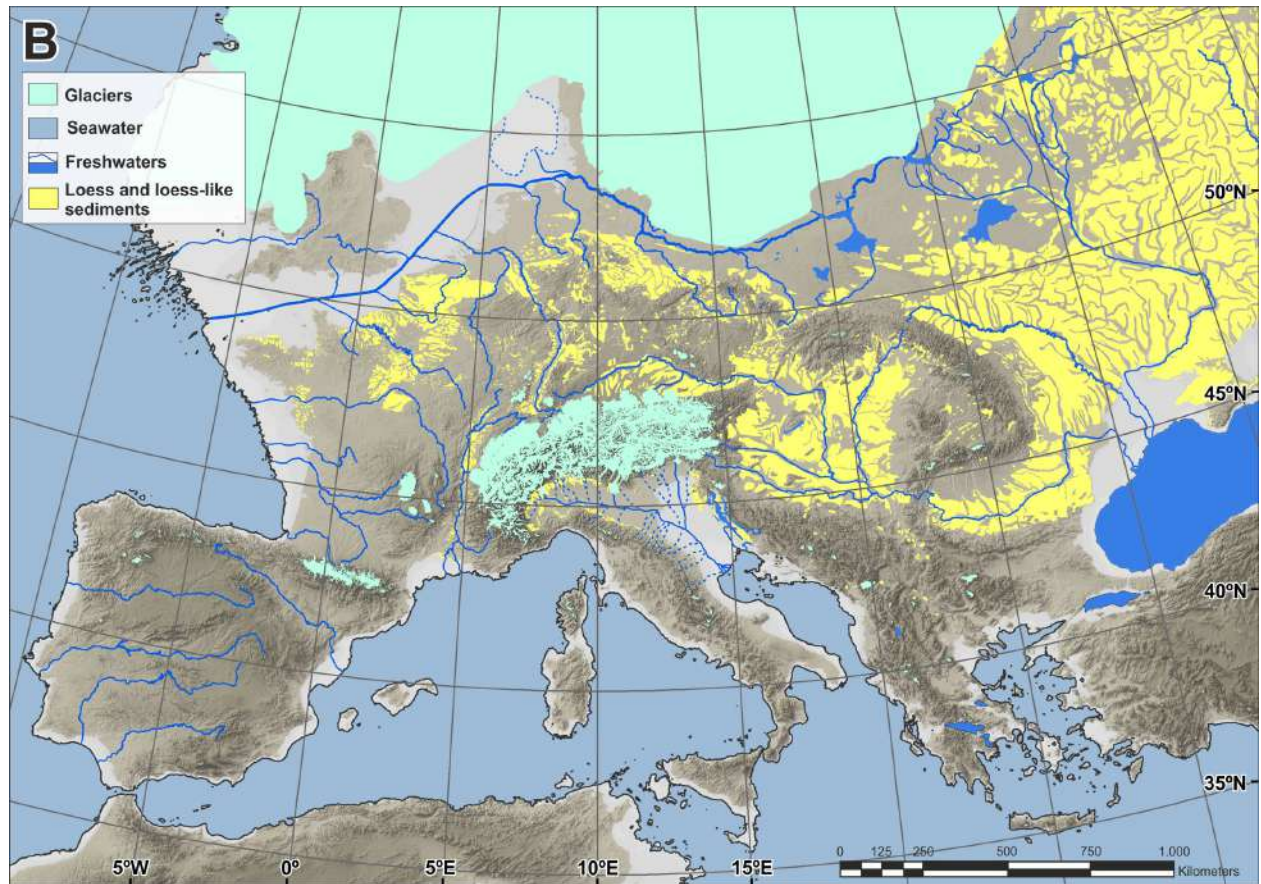Present-day climate: mean annual T: 15ºC; mean annual P: 800 mm

Mediterranean region (Italian peninsula)
Lat.: 42.57˚, Long.: 11.8˚
Elevation: 355 m asl
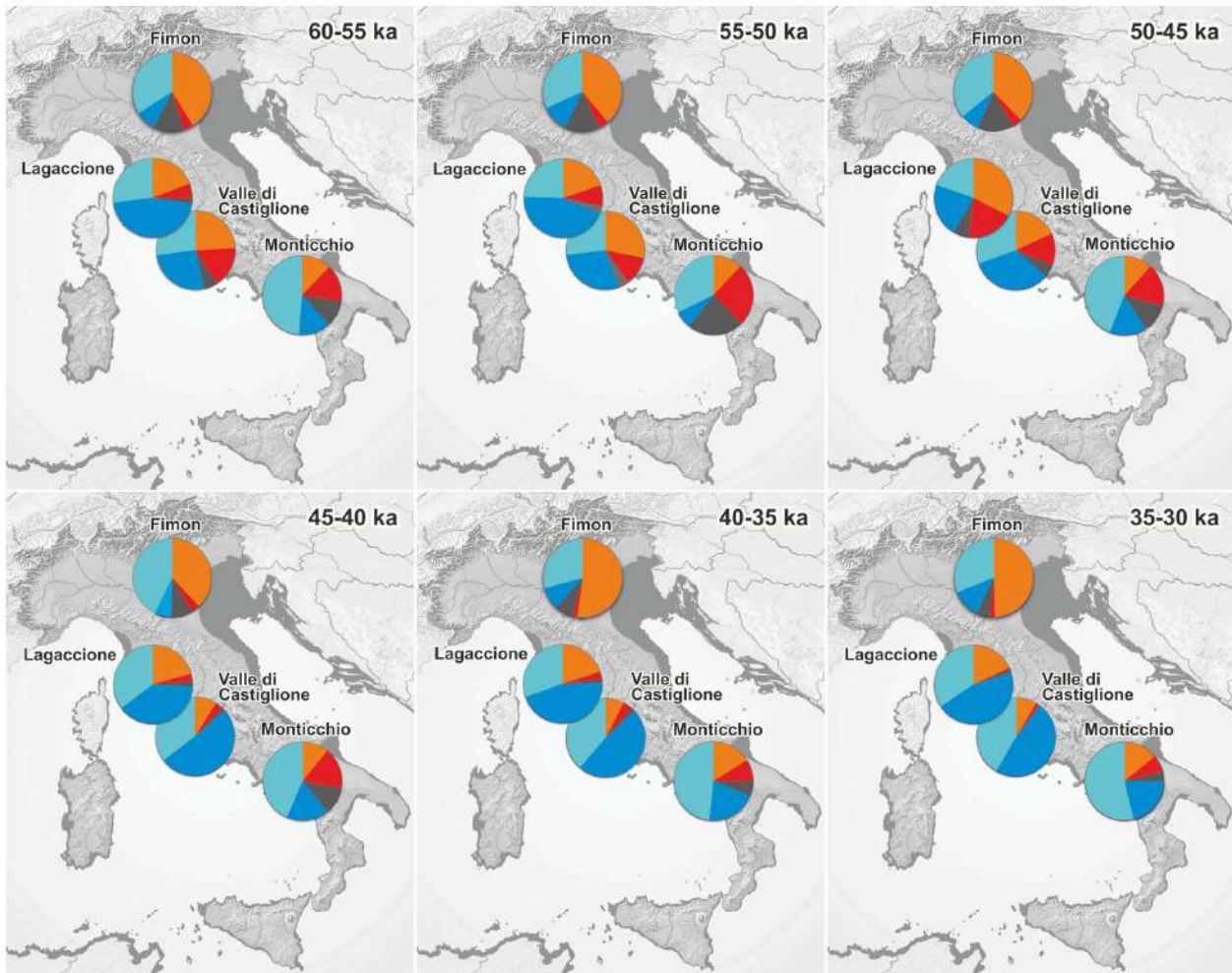Present-day climate: mean annual T: 13.1 °C; maen annual P: 1030 mm

Continental region (north-eastern Italy)
Lat.: 45.46˚, Long.: 11.53˚
Elevation: 23 m asl
Present-day climate: temperate-humid laking a dry season; mean annual T: 12.8 °C; mean annual P: 1038 mm

A

Reconstructed gradients ecogeography within eco-climatic zones

-74   500 1000 1500 2000 2500 Elevation m asl

Tundra zone
Forest - tundra zone (including
Northern side of the Alps)
Southern side of the Alps
Tyrrhenian zone
Atlantic zone
Adriatic basin, Southern Balkan
Peninsula and Circum-Aegean Area
Mid-Southern Iberian Peninsula
Central Anatolian Plateau

Glaciers
Major valley
glaciers (Alps)
Freshwaters
Seawater
Sea level between
-74 and -120 m

50°N
45°N
40°N
35°N

5°W   0°   5°E   10°E   15°E

0   125   250   500   750   1.000
Kilometers
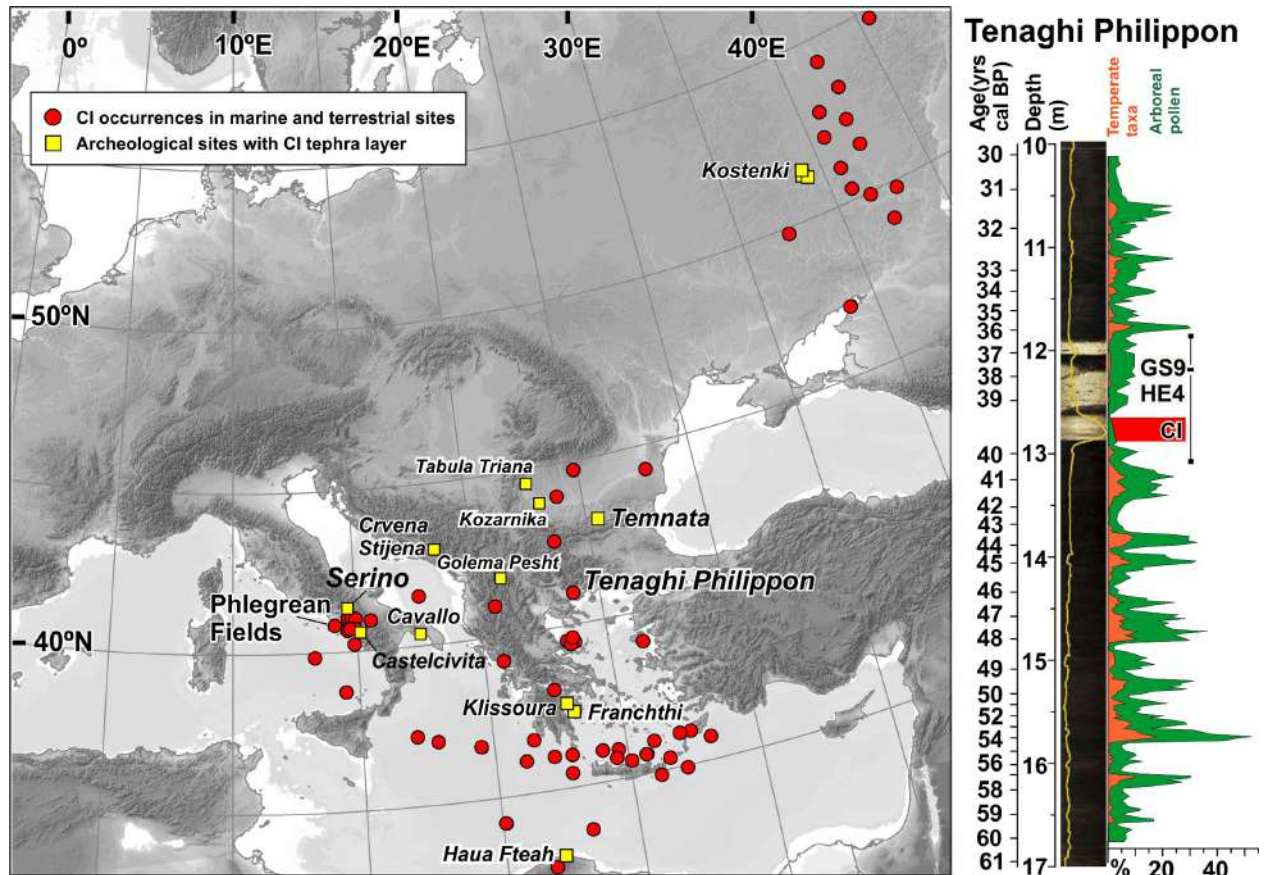
Legend:
- Eurythermic conifers
- Temperate forest
- Other woody taxa
- Xerophytic steppe
- Other herbaceous taxa
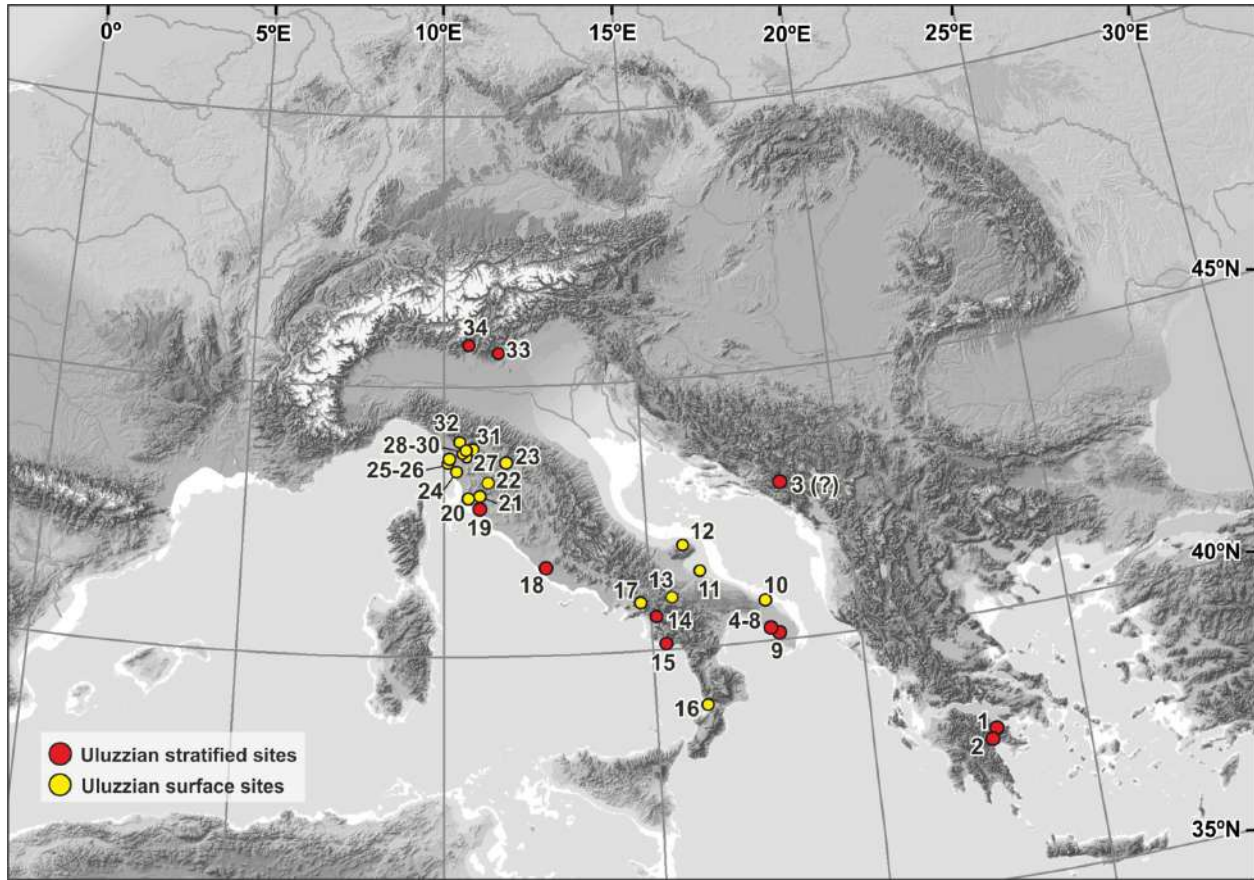
Conflict of Interest and Authorship Conformation Form

Please check the following as appropriate:

- ✓ All authors have participated in (a) conception and design, or analysis and interpretation of the data; (b) drafting the article or revising it critically for important intellectual content; and (c) approval of the final version.

- ✓ This manuscript has not been submitted to, nor is under review at, another journal or other publishing venue.

- ✓ The authors have no affiliation with any organization with a direct or indirect financial interest in the subject matter discussed in the manuscript

    The following authors have affiliations with organizations with direct or indirect financial interest in the subject matter discussed in the manuscript:

Author's name   Affiliation

Sincerely,

On behalf of all authors

Dr. Federica Badino (corresponding author)
federica.badino@unibo.it